



**NAVAL
POSTGRADUATE
SCHOOL**

MONTEREY, CALIFORNIA

THESIS

**SIMULATION OF WIRELESS PROPAGATION IN A
HIGH-RISE BUILDING**

by

Lotfi Boukraa

December 2004

Thesis Advisor:

David C. Jenn

Second Reader:

Tri Ha

Approved for public release; distribution is unlimited.

THIS PAGE INTENTIONALLY LEFT BLANK

REPORT DOCUMENTATION PAGE			Form Approved OMB No. 0704-0188	
Public reporting burden for this collection of information is estimated to average 1 hour per response, including the time for reviewing instruction, searching existing data sources, gathering and maintaining the data needed, and completing and reviewing the collection of information. Send comments regarding this burden estimate or any other aspect of this collection of information, including suggestions for reducing this burden, to Washington headquarters Services, Directorate for Information Operations and Reports, 1215 Jefferson Davis Highway, Suite 1204, Arlington, VA 22202-4302, and to the Office of Management and Budget, Paperwork Reduction Project (0704-0188) Washington DC 20503.				
1. AGENCY USE ONLY (Leave blank)		2. REPORT DATE December 2004	3. REPORT TYPE AND DATES COVERED Master's Thesis	
4. TITLE AND SUBTITLE: Simulation of Wireless Propagation in a High-Rise Building			5. FUNDING NUMBERS	
6. AUTHOR(S) Lotfi Boukraa				
7. PERFORMING ORGANIZATION NAME(S) AND ADDRESS(ES) Naval Postgraduate School Monterey, CA 93943-5000			8. PERFORMING ORGANIZATION REPORT NUMBER	
9. SPONSORING /MONITORING AGENCY NAME(S) AND ADDRESS(ES) N/A			10. SPONSORING/MONITORING AGENCY REPORT NUMBER	
11. SUPPLEMENTARY NOTES The views expressed in this thesis are those of the author and do not reflect the official policy or position of the Department of Defense or the U.S. Government.				
12a. DISTRIBUTION / AVAILABILITY STATEMENT Approved for public release; distribution is unlimited			12b. DISTRIBUTION CODE A	
<p>13. ABSTRACT (maximum 200 words)</p> <p>With the introduction of wireless Local Area Networks (WLANs) in many organizations, it became much easier to intercept confidential files and personal health records. The present study focused on radio frequency propagation in a high-rise building, specifically, the attenuation between floors, and the possibility of intercepting signals through the floors. The current work is based on simulations using the Urbana software tool. It is used to predict the contour of the power levels of signals for a given physical model of the environment using high-frequency ray-tracing methods.</p> <p>The simulation results indicated that the signal levels for a 1 W transmitter could only be detected at the -70 dBm level within two floors (above or below). Even within the two floor range the signal distribution was very nonuniform due to the effects of multipath. The results indicated that closing doors reduced the signal levels, but only slightly for wood doors. Signals escaped the building through the window and were able to travel between floors via this path. The ray tracing accounted for only single diffraction, and therefore rays diffracted two or more times were not included.</p>				
14. SUBJECT TERMS Propagation, Indoor, Wireless, Urbana, propagation between floors, indoor loss			15. NUMBER OF PAGES 97	
			16. PRICE CODE	
17. SECURITY CLASSIFICATION OF REPORT Unclassified	18. SECURITY CLASSIFICATION OF THIS PAGE Unclassified	19. SECURITY CLASSIFICATION OF ABSTRACT Unclassified	20. LIMITATION OF ABSTRACT UL	

THIS PAGE INTENTIONALLY LEFT BLANK

Approved for public release; distribution is unlimited.

**SIMULATION OF WIRELESS PROPAGATION IN A
HIGH-RISE BUILDING**

Lotfi Boukraa
Captain, Tunisian Air Force
B. Eng. (Communication), Ecole de l'Aviation de Borj el Amri, 1996

Submitted in partial fulfillment of the
requirements for the degree of

MASTER OF SCIENCE IN ELECTRICAL ENGINEERING

from the

**NAVAL POSTGRADUATE SCHOOL
December 2004**

Author: Lotfi Boukraa

Approved by: Professor David C. Jenn
Thesis Advisor

Professor Tri Ha
Second Reader

Professor John Powers
Chairman, Department of Electrical and Computer Engineering

THIS PAGE INTENTIONALLY LEFT BLANK

ABSTRACT

With the introduction of wireless Local Area Networks (WLANs) in many organizations, it became much easier to intercept confidential files and personal health records. The present study focused on radio frequency propagation in a high-rise building, specifically, the attenuation between floors, and the possibility of intercepting signals through the floors. The current work is based on simulations using the **Urbana** software tool. It is used to predict the contour of the power levels of signals for a given physical model of the environment using high-frequency ray-tracing methods.

The simulation results indicated that the signal levels for a 1 W transmitter could only be detected at the -70 dBm level within two floors (above or below). Even within the two floor range the signal distribution was very nonuniform due to the effects of multipath. The results indicated that closing doors reduced the signal levels, but only slightly for wood doors. Signals escaped the building through the window and were able to travel between floors via this path. The ray tracing accounted for only single diffraction, and therefore rays diffracted two or more times were not included.

THIS PAGE INTENTIONALLY LEFT BLANK

TABLE OF CONTENTS

I.	INTRODUCTION.....	1
A.	WLAN SECURITY	1
B.	PREVIOUS STUDY	2
C.	OBJECTIVE	2
D.	THESIS OUTLINE.....	3
II.	WIRELESS PROPAGATION BACKGROUND	5
A.	WLAN	5
B.	PROPAGATION.....	6
1.	The Electromagnetic Wave	7
2.	Reflection	8
3.	Diffraction.....	9
4.	Scattering.....	9
C.	THE FREE SPACE MODEL	10
D.	LOSS IN INDOOR ENVIRONMENTS	11
E.	MULTIPATH AND FADING CHANNELS	13
1.	Small-Scale Fading.....	13
2.	Rayleigh Fading	15
3.	Ricean Fading.....	15
F.	ANTENNAS.....	16
III.	SOFTWARE TOOLS.....	19
A.	SOFTWARE TOOLS	19
1.	Cifer Software	20
2.	Xcell Software.....	21
3.	Acad Software	22
4.	Rhino	22
5.	Urbana	23
B.	DESIGN OF THE BUILDING MODEL.....	24
1.	Lobby and Upper Floors	25
2.	Extracting the Edges.....	27
C.	RAY TRACING	28
1.	Geometrical Optics	29
2.	Geometrical Theory of Diffraction.....	29
3.	Ray Tracing.....	30
IV.	URBANA SIMULATION AND RESULTS	33
A.	OBSERVATION POINTS FILE.....	33
B.	PROPAGATION ON A SINGLE FLOOR	33
1.	Open Doors and Windows.....	34
2.	Closed Doors and Open Elevator Shafts.....	36
3.	High-Fidelity Model with Open Doors.....	39
4.	High-Fidelity Model with Close Doors.....	42

C.	PROPAGATION BETWEEN FLOORS OF A HIGH-RISE BUILDING	44
1.	Simulations of a PEC Building	44
2.	Simulation Using a High-Fidelity Building Model.....	53
3.	Transmit Power Level	62
4.	Observation Points in a Vertical Plane	64
D.	SUMMARY	66
V.	CONCLUSION	67
A.	SUMMARY	67
B.	CONCLUSION	67
C.	FUTURE WORK.....	68
APPENDIX.....		69
A.	SAMPLE URBANA INPUT FILE [9]	69
B.	TABLE OF 802.11 SPECIFICATIONS [14].....	72
C.	MATERIAL SPECIFICATION AT 2.4 GHZ [15].....	73
LIST OF REFERENCES.....		75
INITIAL DISTRIBUTION LIST		77

LIST OF FIGURES

Figure 1.	Client and Access point (From Ref. [2].).....	6
Figure 2.	Multiple access points in a building with three floors	6
Figure 3.	Reflection and transmission of a signal through a surface	8
Figure 4.	Diffraction of signal.....	9
Figure 5.	Scattering of electrically small object by a wave.....	10
Figure 6.	Typical path loss in indoor environments (From Ref. [7].)	13
Figure 7.	Small-Scale Fading based on multipath time delay (From Ref. [6].)	14
Figure 8.	Small-Scale Fading based on Doppler spread (From Ref. [6].).....	14
Figure 9.	Antenna patterns (From Ref. [8].).....	17
Figure 10.	Preliminary steps in preparation to running Urbana (From Ref. [9].).....	19
Figure 11.	Interface of Cifer software	20
Figure 12.	Interface of the Xcell software.....	21
Figure 13.	Interface of the Acad software	22
Figure 14.	Interface of the Rhino Software.....	23
Figure 15.	Urbana Input and Output files (From Ref. [9].)	24
Figure 16.	Post-treatment of the Urbana Output file (From Ref. [9].).....	24
Figure 17.	Model of the lobby.....	25
Figure 18.	Model of the first-floor	26
Figure 19.	Walls inside the second-floor.....	26
Figure 20.	Completed model of the twelve story high rise (roof removed to show interior detail).....	27
Figure 21.	Edges of the high-rise model	28
Figure 22.	Example of reflected and diffracted rays	29
Figure 23.	Example of shooting rays for the first floor.....	30
Figure 24.	Model of a single floor.....	34
Figure 25.	Signal contour for all PEC surfaces with open doors and windows	36
Figure 26.	Model of single floor with elevator openings	37
Figure 27.	Signal levels for the case all PEC surfaces with interior doors closed	38
Figure 28.	Floor layout with elevator shafts.....	39
Figure 29.	Signal levels for the high-fidelity model with open doors.....	41
Figure 30.	Signal contour for the high-fidelity model with closed doors	43
Figure 31.	High-rise building model	44
Figure 32.	Signal contour for the first floor lobby (PEC building, open windows transmitter on the seventh floor).....	46
Figure 33.	Signal contour for the second floor (PEC building, open windows transmitter on the seventh floor).....	47
Figure 34.	Signal contour for the third floor (PEC building, open windows transmitter on the seventh floor).....	47
Figure 35.	Signal contour for the fourth floor (PEC building, open windows transmitter on the seventh floor).....	48

Figure 36.	Signal contour for the fifth floor (PEC building, open windows transmitter on the seventh floor).....	48
Figure 37.	Signal contour for the sixth floor (PEC building, open windows transmitter on the seventh floor).....	49
Figure 38.	Signal contour for the seventh floor (PEC building, open windows transmitter on the seventh floor).....	49
Figure 39.	Signal contour for the eighth floor (PEC building, open windows transmitter on the seventh floor).....	50
Figure 40.	Signal contour for the ninth floor (PEC building, open windows transmitter on the seventh floor).....	50
Figure 41.	Signal contour for the tenth floor (PEC building, open windows transmitter on the seventh floor).....	51
Figure 42.	Signal contour for the eleventh floor (PEC building, open windows transmitter on the seventh floor).....	51
Figure 43.	Signal contour for the twelfth floor (PEC building, open windows transmitter on the seventh floor).....	52
Figure 44.	Maximum signal level on each floor inside the building (PEC high-rise building, open windows and the transmitter on the seventh floor).....	52
Figure 45.	High-fidelity building	53
Figure 46.	Signal contour for the first floor (high-fidelity building, open windows transmitter on the seventh floor).....	55
Figure 47.	Signal contour for the second floor (high-fidelity building, open windows transmitter on the seventh floor).....	56
Figure 48.	Signal contour for the third floor (high-fidelity building, open windows transmitter on the seventh floor).....	56
Figure 49.	Signal contour for the fourth floor (high-fidelity building, open windows transmitter on the seventh floor).....	57
Figure 50.	Signal contour for the fifth floor (high-fidelity building, open windows transmitter on the seventh floor).....	57
Figure 51.	Signal contour for the sixth floor (high-fidelity building, open windows transmitter on the seventh floor).....	58
Figure 52.	Signal contour for the seventh floor (high-fidelity building, open windows transmitter on the seventh floor).....	58
Figure 53.	Signal contour for the eighth floor (high-fidelity building, open windows transmitter on the seventh floor).....	59
Figure 54.	Signal contour for the ninth floor (high-fidelity building, open windows transmitter on the seventh floor).....	59
Figure 55.	Signal contour for the tenth floor (high-fidelity building, open windows transmitter on the seventh floor).....	60
Figure 56.	Signal contour for the eleventh floor (high-fidelity building, open windows transmitter on the seventh floor).....	60
Figure 57.	Signal contour for the twelfth floor (high-fidelity building, open windows transmitter on the seventh floor).....	61
Figure 58.	Maximum signal level on each floor inside the high-fidelity building (open windows and the transmitter on the seventh floor).....	61

Figure 59.	Loss between floors for a high-fidelity building (antenna in the first floor, transmit power 1 W)	62
Figure 60.	Signal contour for the seventh floor (1 W source power and antenna on the seventh floor)	63
Figure 61.	Signal contour for the seventh floor (100 mW source power and antenna on the seventh floor)	63
Figure 62.	Vertical signal contour (right view)	65
Figure 63.	Vertical signal contour (left top view)	65

THIS PAGE INTENTIONALLY LEFT BLANK

LIST OF TABLES

Table 1.	Value of n_i in different environments (From Ref. [6].)	12
Table 2.	Input data for the single floor simulation, with open doors and windows.....	34
Table 3.	Responses to input when running $f2f$ for the simulation in Table 2	35
Table 4.	Input data for the single floor simulation, with closed doors	37
Table 5.	Responses to input when running $f2f$ for simulation in Table 4	38
Table 6.	Material specifications for the high-fidelity model	40
Table 7.	Input parameter for the high-fidelity model.....	40
Table 8.	Inputs for running $f2f$ program for the simulation in Table 7	41
Table 9.	Input parameter for the high-fidelity model with closed doors	42
Table 10.	Inputs for running $f2f$ program for the simulation in Table 9	43
Table 11.	Urbana input parameters.....	45
Table 12.	Inputs for running $f2f$ program for the simulation in Table 11	46
Table 13.	Urbana input parameters for the high-fidelity building with realistic materials.....	54
Table 14.	Responses to input for running $f2f$ for the simulation in Table 13	55
Table 15.	Comparison of signal levels for source powers of 1 W and 100 mW	64
Table 16.	Maximum signal level for each of the six vertical planes	66

THIS PAGE INTENTIONALLY LEFT BLANK

ACKNOWLEDGMENTS

I would like to thank my thesis advisor, Dr. David Jenn for his efforts in helping, and supporting to complete this work. Also I would like to thank my family and my friends for their support during my study at the Naval Postgraduate School.

THIS PAGE INTENTIONALLY LEFT BLANK

EXECUTIVE SUMMARY

Wireless communication has become widespread in military operations over the last decade. The development of wireless technology, closely followed by a growing demand for its acquisition, was motivated, in large part, by its efficiency and the relatively low cost of its implementation. With the introduction of wireless Local Area Networks (WLANs) in many organizations, it became much easier to intercept confidential files as military information. Prior to exposing this weakness of wireless networks, studies tended to treat the security problem from two major standpoints. One, which is the subject of this research, was focused on the propagation of radio frequency waves and how to limit the signal area. A second area of research focused on how to prevent unauthorized access by incorporating security features into the network operating systems.

The purpose of this thesis was to continue the study of indoor WLAN propagation. It addressed the problem of WLAN signal distribution in a high-rise building at a frequency of 2.4 GHz (IEEE 802.11b and IEEE 802.11g standard) and examined the effects of changing the local environment on the signal propagation. The present study focused on radio frequency propagation in a high-rise building, specifically, the attenuation between floors, and the possibility of intercepting signals through the floors.

The present work is based on simulations using the Urbana software tool. It was used to predict the contour of the power levels of propagation for a given model using high-frequency ray-tracing methods. The process of building the physical model of the propagation environment, using Rhino is described. When this step is done, the file is saved in *iges* format and then imported to Cifer and converted to a *facet* file, which is the format read by Urbana.

Urbana computes the components of the electric field at observation points provided in a text file with their three-dimensional coordinates (x, y, z) . The simulations included the propagation on one floor, and then proceeded to examine all of the floors of a 12 story high-rise. Two different wall material compositions were examined, all perfect

electric conductor, and more realistic wood and concrete. Both open and closed doors and windows were simulated. Finally the behavior of the signal contours on all floors of the building was compared, as well as the signal distribution in the vertical planes. The simulation results indicated that the signal levels for a 1-W transmitter could only be detected at the -70 dBm level within two floors (above or below). Even within the two floor range the signal distribution was very nonuniform due to the effects of multipath.

The results indicated that closing doors reduced the signal levels, but only slightly for wood doors. Signals escaped the building through the window and were able to travel between floors via this path. The ray tracing accounted for only single diffraction, and therefore rays diffracted two or more times were not included.

I. INTRODUCTION

Wireless communication has become widespread in military operations over the last decade. The development of wireless technology, closely followed by a growing demand for its acquisition, was motivated, in large part, by its efficiency and the relatively low cost of its implementation. A building as military infrastructure with hundreds of offices distributed over several floors requires several miles of wire and weeks of work in order to establish a local area network (LAN). Confronted with the large cost and long installation time, some enterprising system administrators reasoned that the best solution to the problem would be to have a few access points among the various work stations and let users communicate with the network via radio waves. They did this by installing a transmitter and receiver card in each computer in the local network, thus establishing a “wireless” network. The evolution of wireless technology was initially spurred on by advances in digital modulation (i.e., the spread spectrum signal processing technique). Further impetus in the wireless field was generated by advances being made in the way both microelectronic circuits and communication chips were being produced.

A. WLAN SECURITY

With the introduction of wireless local area networks (WLANs) in many organizations, it became much easier to intercept confidential files as military information. The vulnerability of WLANs led to a growing concern among everyone involved with security issues. The most recent computer “hackers” conference, held in Las Vegas in 2004, shows the growing interest in attacking WLAN systems. According to Richard Rushing, chief security officer of AirDefense, “Last year we noted basic denial of service and spoofing attacks, [but] this year hackers have moved on to what we refer to as level three attacks, where hackers are actually injecting traffic into the network and manipulating data” [1]. In other words, hackers are now taking control of wireless systems and granting permission for other people to access the network.

Prior to exposing this weakness of wireless networks, studies tended to treat the security problem from two major standpoints. One, which is the subject of this research, focused on the propagation of radio frequency waves and how to limit the signal area. A

second area of research focused on how to prevent unauthorized access by incorporating security features into the network operating systems.

B. PREVIOUS STUDY

This research was concerned with the question: what is the distribution and levels of signals radiated by WLANs, and can they be intercepted by unauthorized users?

Earlier phases of this research, carried out by Sumagaysay [2], studied indoor propagation by using the **Urbana** software tool. Sumagaysay concluded that an effective measure to cut down on unwanted interception of wireless network data was to locate the access points in the most interior parts of the building. This was followed by trying to “close all doors,” i.e, ways of containing the radiation. Next, special types of blinds were installed over the windows. Finally the system’s antenna coverage was limited and directed toward the interiors of the building. These simple measures were shown to be effective in reducing the WLAN signals outside of the building.

Another study looked at the security problem associated with point-to-point wireless systems. Lim [3] showed that using narrow antenna beams in point-to-point systems can limit the interception of the signal.

C. OBJECTIVE

The purpose of this thesis was to continue the study of indoor WLAN propagation. It addressed the problem of WLAN signal distribution in a high-rise building at a frequency of 2.4 GHz (IEEE 802.11b and IEEE 802.11g standard) and examined the effects of changing the local environment on the signal propagation. The present study focused on radio frequency propagation in a high-rise building, specifically, the attenuation between floors, and the possibility of intercepting signals through the floors. Also, it compared the results with some of the earlier work focused on enhancing the security of WLAN systems. The present work was based on simulations using the **Urbana** software tool. It is used to predict the contour of the power levels of propagation for a given model using high-frequency ray-tracing methods.

D. THESIS OUTLINE

Following the Introduction, Chapter II describes the basic theory behind wireless propagation, in general, and more specifically in the indoor environment. Chapter III describes the different software applications used in this research and the design of the physical models of the environments used in the simulations. Chapter IV describes the various simulations and shows the results obtained. Chapter V contains both concluding comments and recommendations for future research. The Appendix contains a sample Urbana input file, a table of the specifications for the IEEE 802.11 standards and a table of material specifications.

THIS PAGE INTENTIONALLY LEFT BLANK

II. WIRELESS PROPAGATION BACKGROUND

A wireless network enables people to communicate information from one point to another without any physical connection by using radio frequency (RF) waves. In this chapter different configurations of wireless local area networks and the basic phenomenon of the radio frequency signal propagation are discussed.

A. WLAN

When transmitted data are encoded into signals, which are amplified so that they have enough energy to reach receivers which might be far from the transmission point. In a typical configuration, a transmitter–receiver (called the access point) is connected to the wired network using standard cable. Signals from users are transmitted and received using wireless cards. A typical access point can cover from two to five hundred feet, thus allowing access for 15 to 50 users.

Wireless network configurations range from simple to highly complex. A connection can be established between any two personal computers (PCs) adapted with wireless cards. This kind of connection is called a “peer-to-peer” ad-hoc connection, giving each user access to the resources of the other computer, even in the absence of a central server or internet network. Such a connection does not require any unique configuring or identification to access the other computer.

There is a second type of connection using a single access point (Figure 1) that is more common than the one described above. Depending on the topology of the network being used, various different configurations may be found. The most common configuration has only one access point which is connected to the server/internet network through a regular wired connection. Users can access the network by connecting their PCs to the access point. The access point and the client’s PC transmit and receive data using radio frequency signals.



Figure 1. Client and Access point (From Ref. [2].)

Since the practical range for an access point usually does not exceed five hundred feet, larger indoor environments, like those found in some universities and companies, need more than one access point. Figure 2 displays designs which allow for larger coverage areas and buildings having many floors.

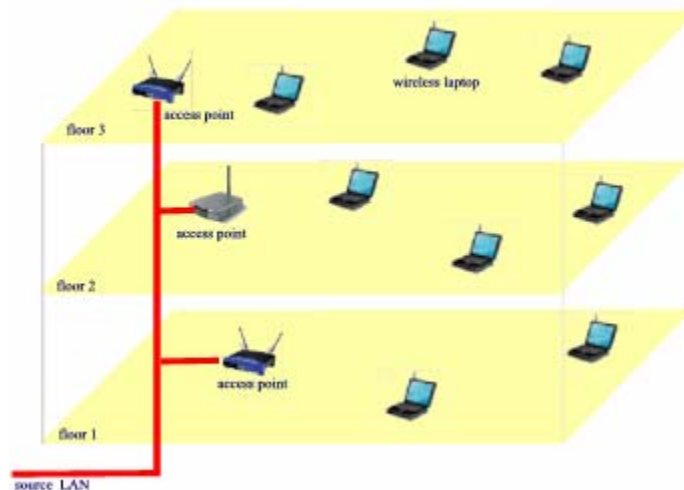


Figure 2. Multiple access points in a building with three floors

B. PROPAGATION

In indoor environments electromagnetic waves propagate in complex paths due to the presence of many different scatters. Wireless signals are like any other radio frequency signals, in that they are altered by the multiple effects of reflection, diffraction and scattering.

1. The Electromagnetic Wave

The basic electromagnetic plane wave has a simple association between its periodic sinusoidal electric and magnetic field vectors, which are perpendicular to each other and the direction of the propagation. In free space, electromagnetic waves travel at the speed of the light ($c = 3 \times 10^8$ m/s). The interaction of a wave and material is affected by the material properties, such as conductivity (σ), permittivity (ε), permeability (μ), and resistivity (R_s). Since the vast majority of the material in an indoor or urban setting are nonmagnetic, it will be assumed from here on that

$$\mu = \mu_0 \quad (1)$$

where $\mu_0 = 4\pi \times 10^{-7}$ (H/m) is the permeability of free space.

Another property of the material is its complex permittivity, defined as the relationship between the electric displacement and the electric field intensity [4]. Consideration of this constant accounts for heat loss in the medium due to the damping of the vibration dipole moments and is defined as

$$\varepsilon = \varepsilon' - j\varepsilon'' = \varepsilon_0 \varepsilon_r \left(1 - j \frac{\sigma}{\omega \varepsilon_0 \varepsilon_r} \right) = \varepsilon_0 (\varepsilon'_r - j\varepsilon''_r) \quad (2)$$

where ε is the complex permittivity,

σ is the conductivity of the material (S/m),

$\varepsilon_0 = 8.8542 \times 10^{-12}$ (F/m) is the free space permittivity,

ε_r is the relative permittivity of the material,

ε'_r and ε''_r are the real and imaginary parts of the relative permittivity, and

ε' and ε'' are the real and the imaginary parts of the complex permittivity.

The phase velocity of the radio frequency wave inside the material is a function of its permittivity and permeability parameters. In free space the velocity is

$$v = \frac{1}{\sqrt{\varepsilon_0 \mu_0}} = c. \quad (3)$$

In any other medium the velocity will be

$$v = \frac{1}{\sqrt{\epsilon' \mu'}} = \frac{1}{\sqrt{\epsilon_0 \epsilon_r \mu_0 \mu_r}} = \frac{c}{\sqrt{\epsilon_r \mu_r}} \quad (4)$$

where v is the phase velocity of the wave in the material and c is the velocity in free space.

2. Reflection

Reflection occurs when a radio wave impinges on a surface. As shown in Figure 3, some energy is reflected at the surface while some of it is transmitted [4]. By Snell's law the angle of reflection is equal to the angle of incidence. In an urban setting RF waves propagate in several different directions and encounter many reflecting surfaces. By successive reflections, a signal source can reach a station or an access point by taking a variety of different paths. The amount of reflection depends upon several factors, such as: 1) the frequency of the signal, 2) the angle of incidence, 3) the reflecting properties of the surfaces (among other things, determined by its material, geometry, and thickness). A "perfect" electric conductor (PEC) is one that suffers no energy loss through reflection. However, in the vast majority of dielectric surface materials (wood, concrete, glass, etc.), at least part of the incident energy is reflected and the remainder transmitted.

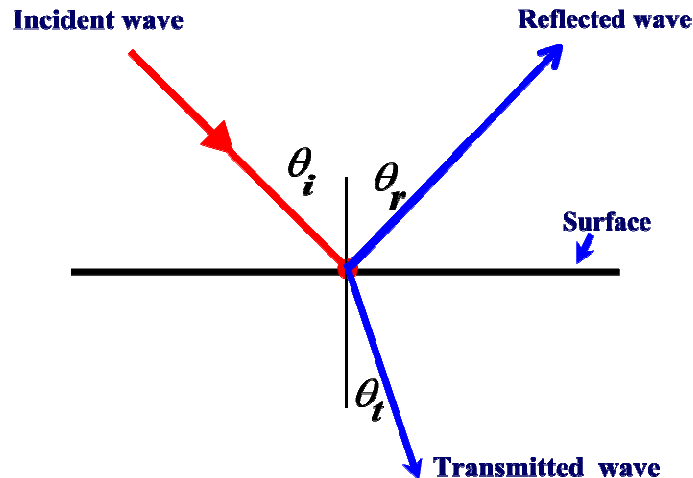


Figure 3. Reflection and transmission of a signal through a surface

3. Diffraction

When electromagnetic waves travel through the air and strike the discontinuities in impenetrable obstacles (Figure 4), a secondary wave is created behind the surface of the point of contact. This phenomenon, called diffraction, is very common in indoor environments due to the presence of many edges and corners [4]. The amount of diffraction is a function of the geometry of the surfaces and the characteristic of the RF signal (such as amplitude, phase, and polarization).

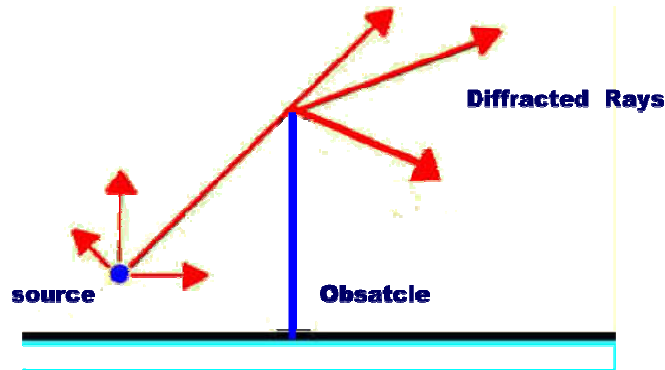


Figure 4. Diffraction of signal

4. Scattering

Scattering occurs when the wave strikes an object that is small relative to the wavelength, resulting in propagation in many directions [4]. For objects having the dimensions much smaller than the wavelength, the scattering is described by Rayleigh scattering. Small objects scatter more or less uniformly in all directions, as shown in Figure 5. In indoor environments typical scattering objects range in size from small desk tools (like pens)—two to three centimeters in length, to the size of furniture and humans (from one to three meters in length). Compared to the wavelength at 2.4 GHz (12.5 cm), these dimensions place all of these objects in the Mie-scattering region or the optical region [5].

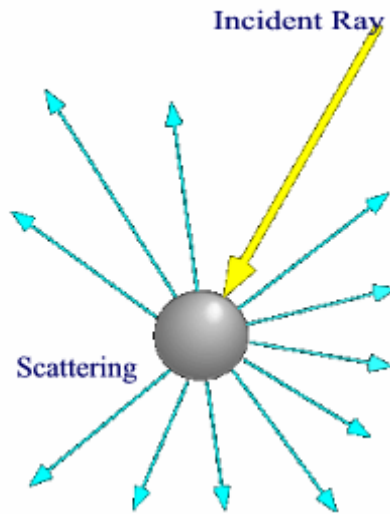


Figure 5. Scattering of electrically small object by a wave

C. THE FREE SPACE MODEL

The Friis transmission formula is used to approximate the power received over a free space transmission path when the transmitter and the receiver are in each other's line of sight and there are no obstructions between them [4]. The power received is related to the transmitted power according to the following equation:

$$P_r = \frac{P_t G_t G_r \lambda^2}{(4\pi)^2 d^2 L} \quad (5)$$

where P_r is the power out of the receiving antenna (W),

P_t is the power transmitted (W),

G_t is the gain of the transmission antenna,

G_r is the gain of the receptor antenna,

$\lambda = c/f$ is the wavelength of the signal,

d is the distance between the transmitter and the receiver, and

L is a total system loss factor.

The power of the RF signal decreases as the distance from the access point increases. This loss is proportional to the square of the distance. The received power is influenced by the frequency of the signal. When the frequency of the signal is low, material attenuation is less than for higher frequencies. In such cases, the RF signal may be able to permeate walls easily, whereas when the frequency of the wave is in the high range, the inverse is true. To avoid compromising the integrity of an indoor network, antennas with a high gain are frequently used. The gain can be determined from the following equation

$$G = \frac{4\pi A_e}{\lambda^2} \quad (6)$$

where A_e is the effective aperture (m^2).

D. LOSS IN INDOOR ENVIRONMENTS

Losses in an indoor environment are usually due to the presence of objects with lossy materials, such as wood, plastic and furniture, as well as the presence of people. All of these contribute to the loss of a signal's energy by reflection, diffraction and absorption. The loss between the end points of a link can be identified by measuring the difference between the transmitted power at the output of the transmitter and the power received at the input of the receiver. Assuming $L = 0$ (no system losses), the path losses is

$$\text{PL}[\text{dB}] = 10 \times \log\left(\frac{P_t}{P_r}\right) = -10 \times \log\left(\frac{G_t G_r \lambda^2}{(4\pi)^2 d^2}\right). \quad (7)$$

For an isotropic antenna, where the gain is one, the path loss is referred to as the free space path loss

$$\text{PL}_{ref}[\text{dB}] = 10 \times \log\left(\frac{P_t}{P_r}\right) = -10 \times \log\left(\frac{\lambda^2}{(4\pi)^2 d^2}\right). \quad (8)$$

Note that at 2.4 GHz, $\lambda = 0.125$ m. Therefore the path loss at 1 m is 40 dB and at 10 m it is 60 dB.

The general equation for the line-of-sight path loss, also referred to as the Log distance path loss model, is given by the following equation [7]:

$$PL[\text{dB}] = PL_{ref}[\text{dB}] + n_1 10 \log d \quad (9)$$

where $PL_{ref}[\text{dB}]$ is the free space loss in dB given by Equation (8) calculated at $d = 1 \text{ m}$ and n_1 is a correction factor computed from the collection of empirical data (as defined in Rappaport [6]). Table 1 shows n_1 for certain environments.

Environment	n_1
Free space	2
Urban Area	2.7 – 3.5
Shadowed Urban Area	3 – 5
Indoor Loss	1.6 – 1.8

Table 1. Value of n_1 in different environments (From Ref. [6].)

Figure 6 shows the typical variation of path loss in an indoor environment as a function of the distance between the receiver and the transmitter. The first segment in Figure 6 is essentially the line-of-sight free space rate of attenuation. The two other segments show that higher levels of attenuation occur due to obstructions and scattering. The abrupt drop at 1000 feet is due to blockage.

Walls are often different in texture from one side of a room to the other (and different between buildings), creating unique characteristics which influence wave propagation. Also, the behavior of waves change over time, i.e., their properties at a given time are dependent upon their position relative to moving objects causing scattering.

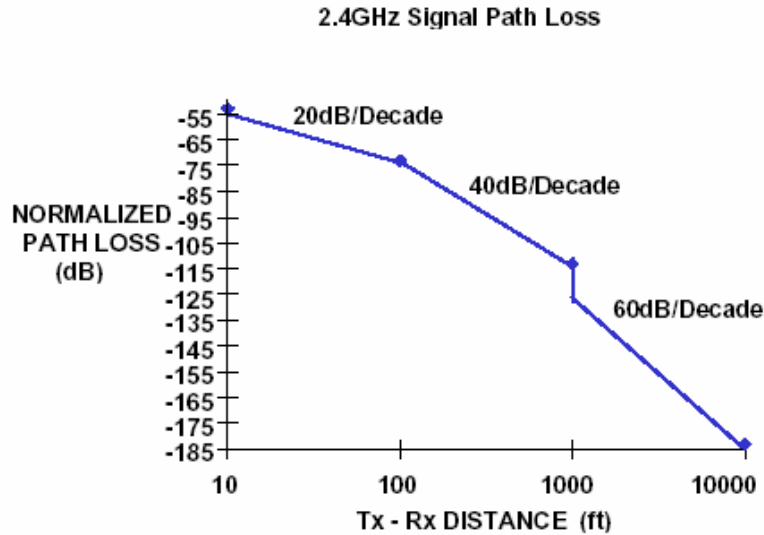


Figure 6. Typical path loss in indoor environments (From Ref. [7].)

E. MULTIPATH AND FADING CHANNELS

In wireless environments, waves transmitted through the air follow different paths, thus reaching the receiver at different times. A measure of the range of time over which the signal arrives is the delay spread parameter. Signals may also encounter frequency variation due to the Doppler shift induced by the motion of the transmitter, receiver, or scatter. The wave components also have different amplitudes and phases [6].

There are generally two major types of multipath fading, large-scale fading and small-scale fading. Whereas large-scale fading occurs over relatively large distances between the transmitter and the receiver, small-scale fading refers to fading that occurs over shorter distances (a few wavelengths). Small-scale fading potentially has more detrimental effects on the signal than does large-scale fading [6].

1. Small-Scale Fading

All indoor wireless systems demonstrate small-scale fading characteristics. This has two main effects, the time it takes to disperse and the time variance of the waves through different paths created by the Doppler shift frequency. The first category of small-scale fading, referred to as time dispersion, or spreading, is divided in two categories, flat fading and frequency selective fading, as illustrated in Figure 7.

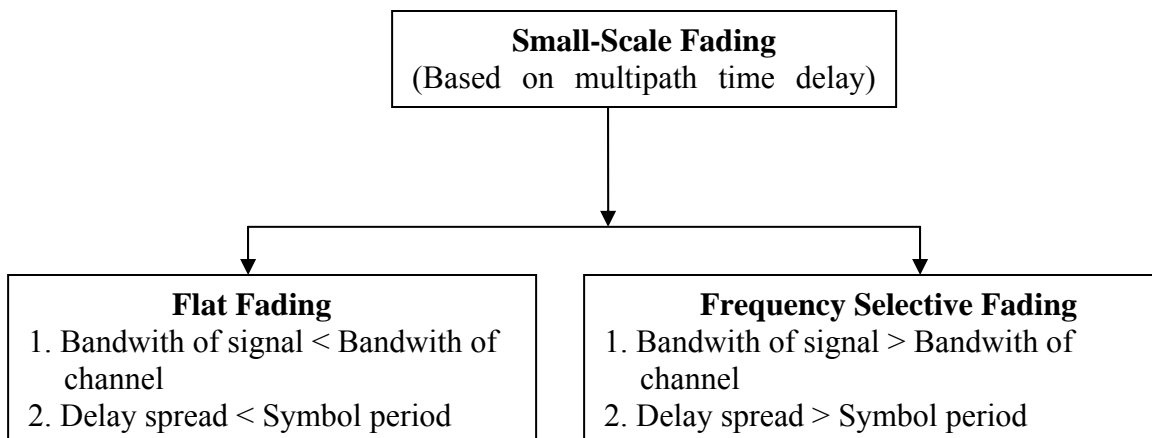


Figure 7. Small-Scale Fading based on multipath time delay (From Ref. [6].)

The second effect of the time variance due to the Doppler spread is divided into either fast fading or slow fading, as shown in Figure 8. For fast fading channels, the channel impulse response change is relatively fast compared to the baseband signal variations. On the other hand, if the change is slower, then the channel is categorized as slow fading [6].

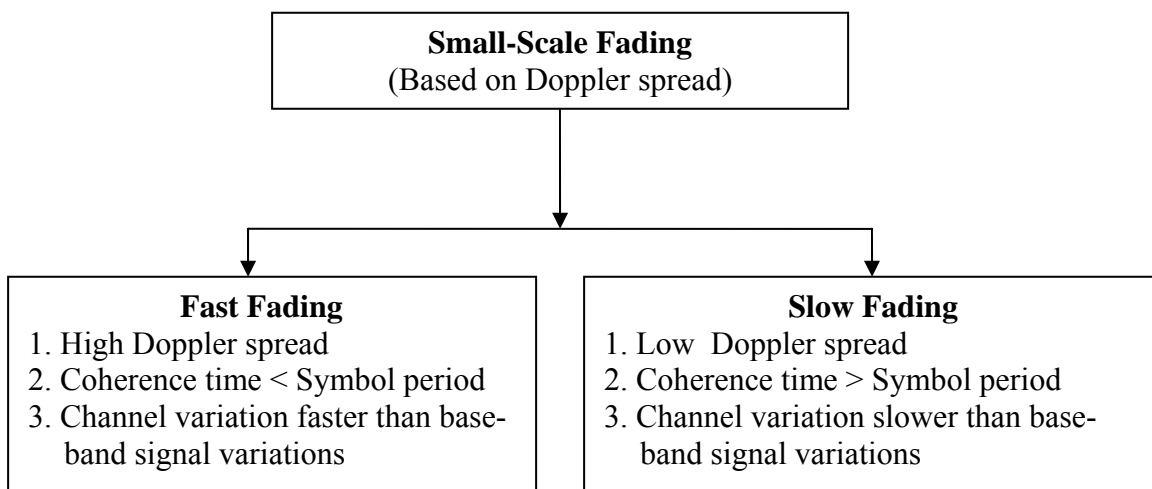


Figure 8. Small-Scale Fading based on Doppler spread (From Ref. [6].)

Most indoor environments experience both slow and fast fading due to the movements of people inside (this can be either slow or fast, depending on their distance from the source and the velocity and direction of movements). Also, the presence of certain

moving parts or equipment, such as fans, may cause fast fading. Because of the large number of scattering sources and their uncorrelated amplitude and phase, statistical methods are an appropriate approach to modeling the propagation path. The most common of such models are the Rayleigh fading model and the Ricean model, discussed next.

2. Rayleigh Fading

The Rayleigh model is especially helpful when the direct path between the transmitter and the receiver is blocked, like it is between the floors of a building, or inside an office [6]. The probability density function (PDF) is given by [6]

$$p(r) = \begin{cases} \frac{r}{\sigma^2} \exp\left(-\frac{r^2}{2\sigma^2}\right) & 0 \leq r \leq \infty \\ 0 & r < 0 \end{cases} \quad (10)$$

where r is the magnitude of the signal voltage and σ is the standard deviation of the received voltage signal.

3. Ricean Fading

Ricean fading occurs where the line-of-sight between the transmitter and the receiver is unobstructed. The probability density function is given by the following equation [6]:

$$p(r) = \begin{cases} \frac{r}{\sigma^2} e^{-\frac{(r^2+A^2)}{2\sigma^2}} I_0\left(\frac{Ar}{\sigma^2}\right) & A \geq 0, r \geq 0 \\ 0 & r < 0 \end{cases} \quad (11)$$

where A is the amplitude of the peak of the dominant signal (usually the line-of-sight path) and I_0 is the modified Bessel function of the first kind, zero order.

F. ANTENNAS

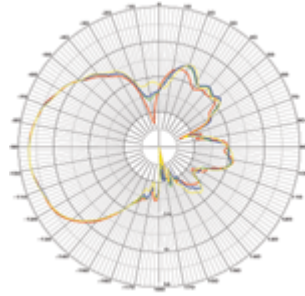
Antennas are the means by which electromagnetic waves are excited and received in space. An isotropic antenna is characterized by a uniform radiation pattern in all directions. Isotropic antennas are used as a reference by which to evaluate more practical antennas. In different wireless domains, including those in indoor environments, different types of antennas are used to satisfy the needs of users. They are tailored to the specific geometry of the environment in question [4]. The following are some important characteristics of antennas:

- Directivity - This is equal to the ratio of the maximum power radiated to the average power radiated.
- Efficiency - A signal will be weakened due to the mismatch between the waveguide and the antenna, or due to dielectric and ohmic losses of the antenna.
- Gain - The gain is the product of the directivity and the efficiency; when the efficiency is 100%, the gain is equal to the directivity.
- Polarization - This refers to the direction of the electric field vector radiated by the antenna. For wireless applications polarization is generally linear (either vertical or horizontal).
- Pattern - This is the graphical representation in three-dimensional space of the gain as a function of the angular direction. Most antennas used in WLAN systems have a pattern with a main lobe and some side lobes.

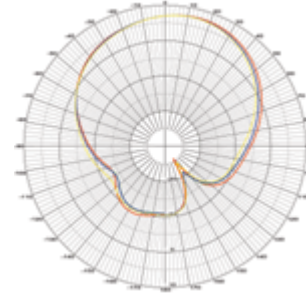
Figure 9 shows a directional patch antenna that is linearly polarized and designed to work from 2.400 to 2.483 GHz. It may be mounted on a wall or on the ceiling. Figure 9 (b) shows the horizontal plane pattern, and Figure 9 (c) shows the vertical plane pattern.



(a)



(b)



(c)

Figure 9. Antenna patterns (From Ref. [8].)

This chapter focused on the background theory behind wireless propagation in an indoor environment and discussed some of the system issues. The following chapter presents the software used in this work and the steps taken to design the building model.

THIS PAGE INTENTIONALLY LEFT BLANK

III. SOFTWARE TOOLS

The purpose of this research was to predict the propagation of wireless RF signals in an indoor environment under different situations. This chapter will focus on different software used to accomplish this work and the different steps to design a physical indoor model.

A. SOFTWARE TOOLS

In order to accomplish this goal, software tools are required to generate the scattering model for the environment in question. A great number of software applications are potential candidates for this purpose, such as **AutoCad** (by Autodesk, Inc.), and the Advanced Computer Aided Design System or **Acads** (by Lockheed Martin). A third computer aided design (CAD) package is **Rhinoceros** (or **Rhino**).

Once the scattering model is generated, **Urbana** is used to calculate the signal contours. **Urbana** is actually a collection of software applications that include **Cifer** and **Xcell**. These will be discussed in the following sections. The diagram in Figure 10 shows the sequence of steps that take one from building the model, converting it to a *facet* file so it can read by **Urbana**, to extraction of the edges, and finally to the creation of the observation points file.

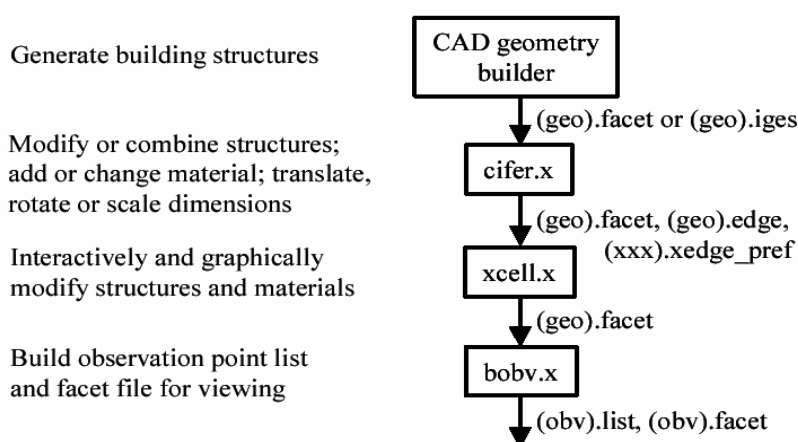


Figure 10. Preliminary steps in preparation to running **Urbana** (From Ref. [9].)

1. Cifer Software

Cifer is a utility that was developed in 1998 at the University of Illinois in Urbana-Champaign. **Cifer** is used to convert *iges* input files from CAE applications into *facet* files. It can also be used to check the accuracy and validity of the files created. Subsequent to 1998, many features have been added, such as creating a new geometry, changing surface materials, extracting edges from a *facet* file, and basic features like translation, rotation, and scaling. **Cifer** also allows one to combine two *facet* or *edge* files into a single file of the same type. Figure 11 shows the graphical user interface (GUI) of the **Cifer** software used for the translation of an *iges* file into *facet* file.

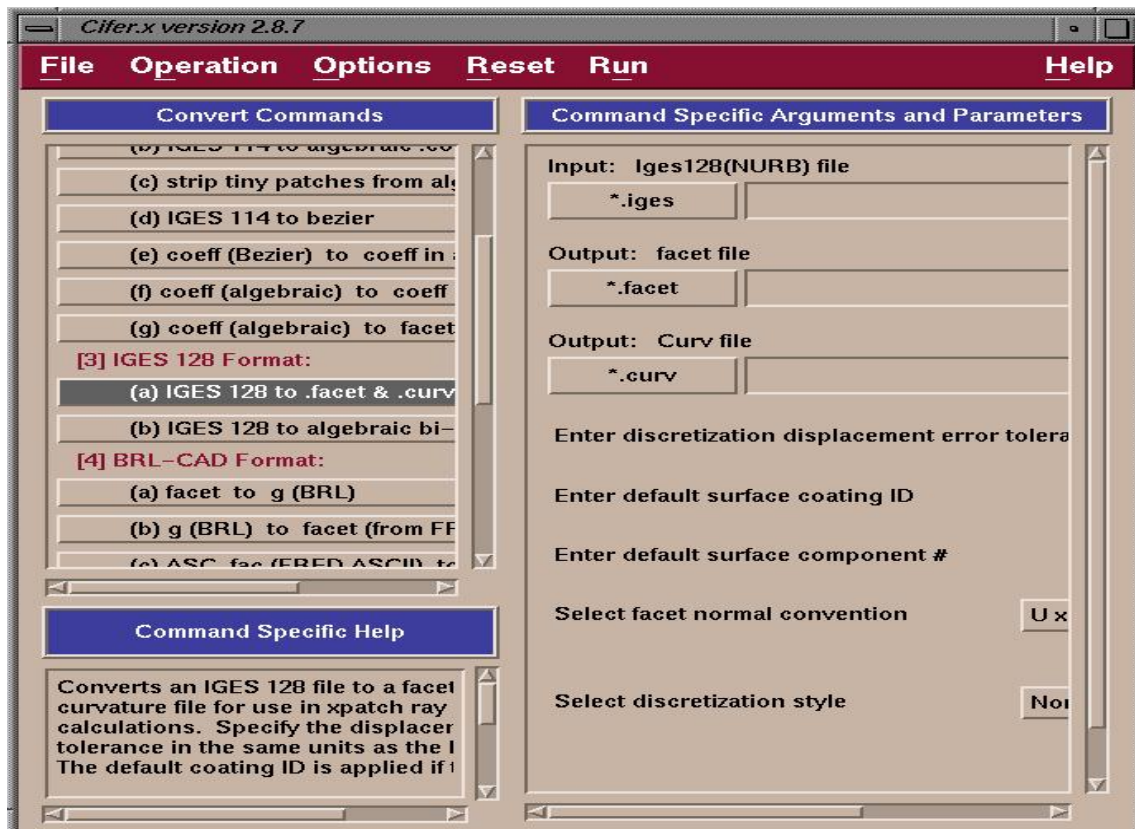


Figure 11. Interface of **Cifer** software

2. Xcell Software

Xcell is another application in the **Urbana** package, which allows editing and viewing of *facet* files, or *edge* files. **Xcell** is used to visualize a *facet* file in the graphic window, creating a basic operation within the graphic environment (facilitating such operations as translation, rotation, zooming in or out, etc.). It also allows one to display *facet* files with *edge* files and *antenna* files, all in the same window.

Another feature of **Xcell** is the option to generate ray trajectories. This can be accomplished by setting the antenna parameters and propagation options appropriately. The results allow one to preview the form of wave propagation in the model. **Xcell** also has the capability to verify that the *facet* files of the model are all as expected, i.e., that there is no discrepancy in converting *facet* to *iges* file format. This enables one to use the ray tracing option as the first step in checking the opacity of the tested model. Figure 12 show an interface of the **Xcell** software.

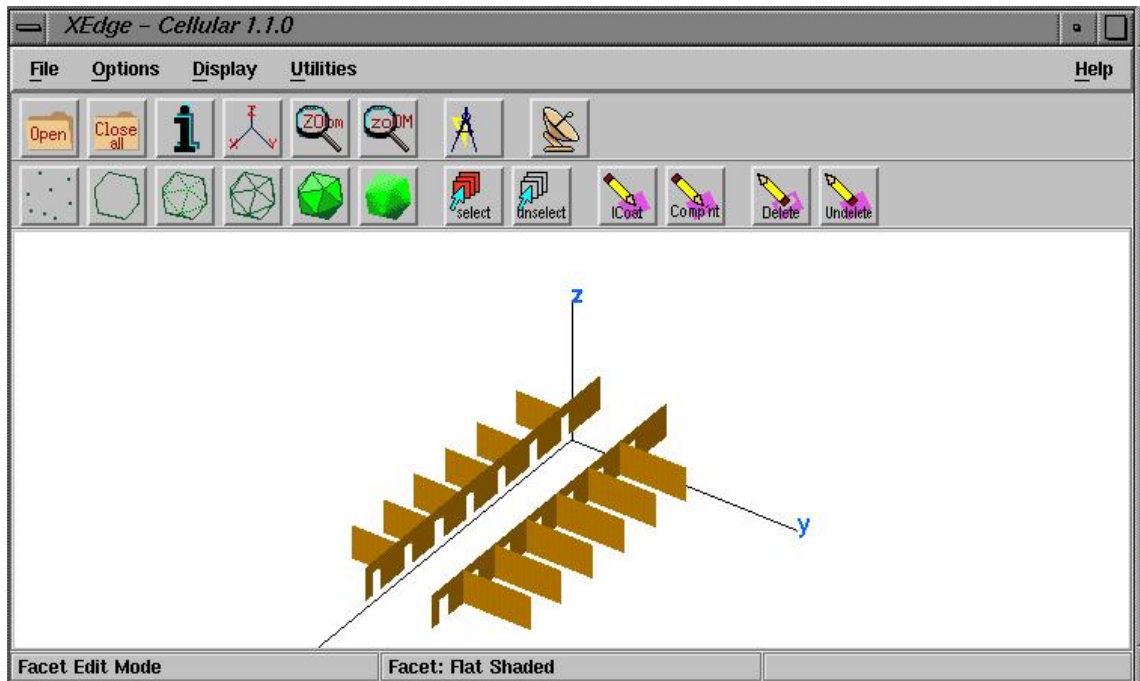


Figure 12. Interface of the **Xcell** software

3. Acad Software

Acad is a CAD package with many of the capabilities of the more commonly known **AutoCad**. It was specifically designed to be used in tandem with **Urbana**. In particular, it does the triangular facetization of the geometry surfaces. **Acad** is compatible with different file formats, such as *facet*, *iges*, and *ascii* formats.

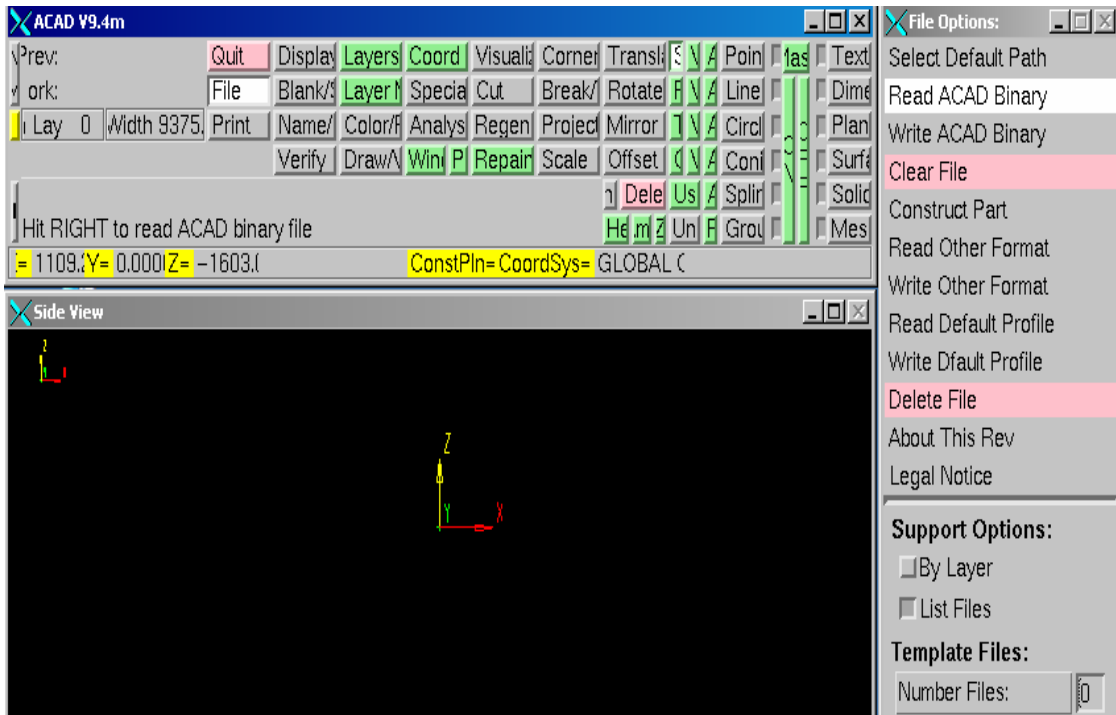


Figure 13. Interface of the **Acad** software

4. Rhino

Rhino is a very powerful CAD software package for Windows platforms. **Rhino** can create, edit, analyze and translate curves, surfaces and solids. Not complex to use, nor limited by the degree or size of the environment under study, **Rhino** is well-suited to the design of prototypes. **Rhino** is compatible with most drawing programs. **Rhino**'s features include a file format that supports *iges*, *dwg*, *vrml*, *bmp*, *jpg* and others. Figure 14 shows a **Rhino** window.

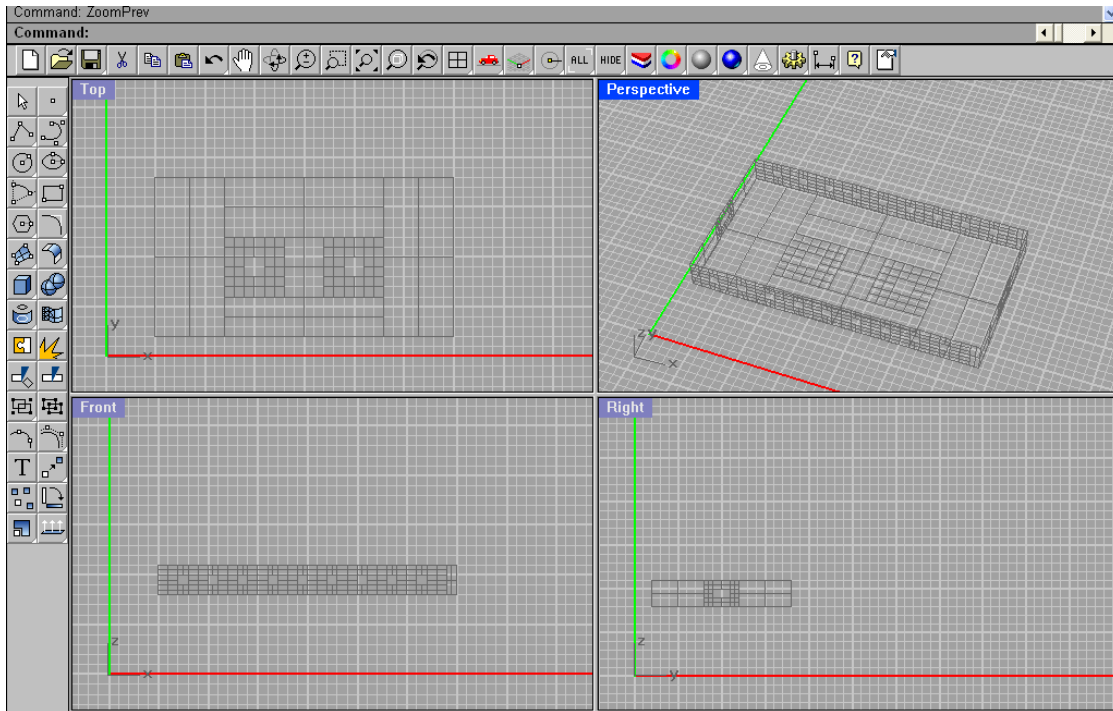


Figure 14. Interface of the Rhino Software

5. Urbana

Urbana is software developed at the University of Illinois. **Urbana** is used to simulate the propagation of electromagnetic waves in a given model. The model could be just a room or office, or it could be a large building, or even a whole city (with many different buildings). **Urbana** uses geometrical optics, physical optics, and the geometric theory of diffraction for computing the electromagnetic field at a given set of points. Different types of antennas can be selected or the user can provide a pattern file for other antennas types. All of the information required for **Urbana** to run a simulation is specified in an input file, which must have a file name extension *ur_input*. Appendix A is an example of an input file. The process of running **Urbana** is shown in Figure 15.

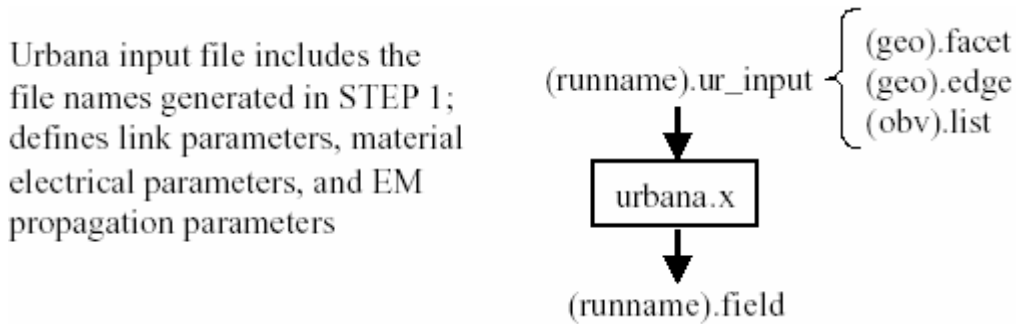


Figure 15. **Urbana** Input and Output files (From Ref. [9].)

Once **Urbana** completes the simulation, it is necessary to use the *f2f* program or the *f2fd* program to convert the output from a *field* file to a *facet* file, allowing one to view it in **Xcell**. The **Urbana** data is converted into a colored *facet* file containing the total electric field level. This part of the process is illustrated in Figure 16.

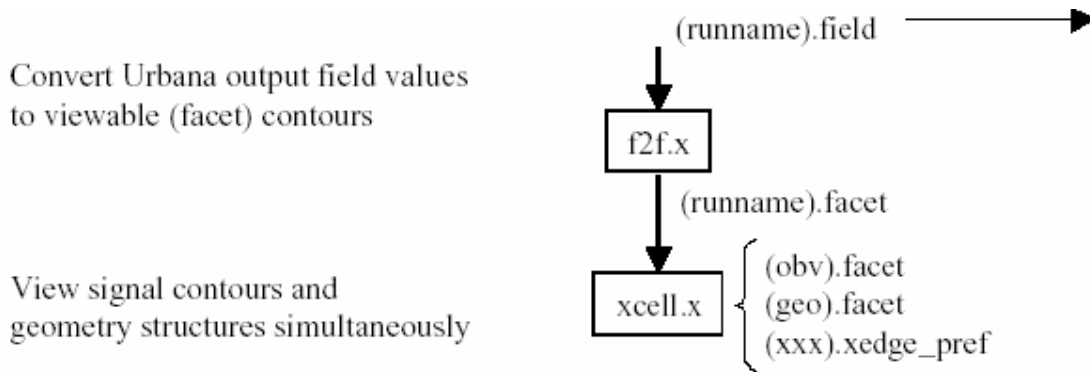


Figure 16. Post-treatment of the **Urbana** Output file (From Ref. [9].)

B. DESIGN OF THE BUILDING MODEL

Prior to feeding the data into **Urbana** for simulation, it is necessary to first build a model of the environment with the appropriate fidelity. This can be done using tools like **Cifer**, **Acads** or **Rhino** as discussed in Section A. The model is constructed as a set of surfaces that are joined in such a way that a “block,” or floor of the building is formed. Each block is built separately in order to better facilitate a modular design (i.e., the block model is intended to be used more than once in a structure). The **Rhino** program was used to design the different blocks or floors of the building.

1. Lobby and Upper Floors

The first section designed was the ground floor lobby of a hypothetical hotel or office building. This lobby has four side walls, with a few windows and a large door. The dimensions of the lobby model are shown in Figure 17.

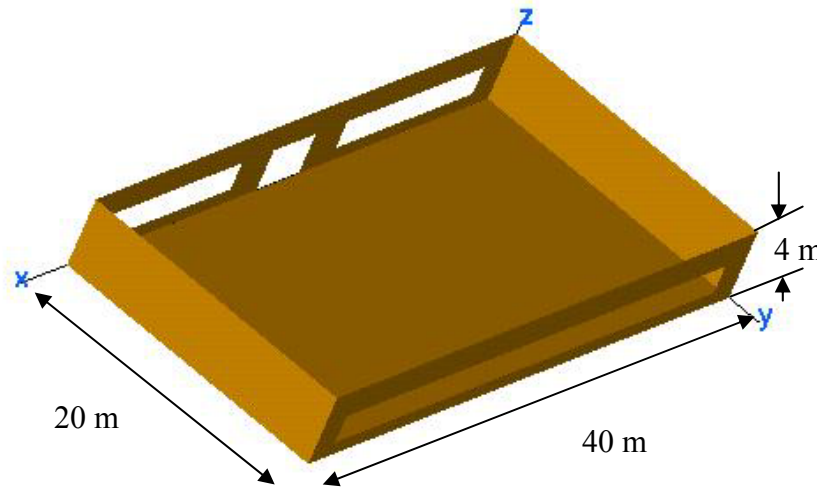


Figure 17. Model of the lobby

The second floor has a smaller area than the lobby. Here, two square holes in the floor are added for elevators, which will be in the actual design of any building. The dimensions of this floor are shown in Figure 18. The material assigned to both the lobby and the first-floor models is $icoat = 1$, a material that is the approximate equivalent to a concrete-type material (as the physical and electrical characteristics of concrete are described in the next chapter). The windows are assigned a value that is $icoat = 2$ correspond to the characteristic of the glass.

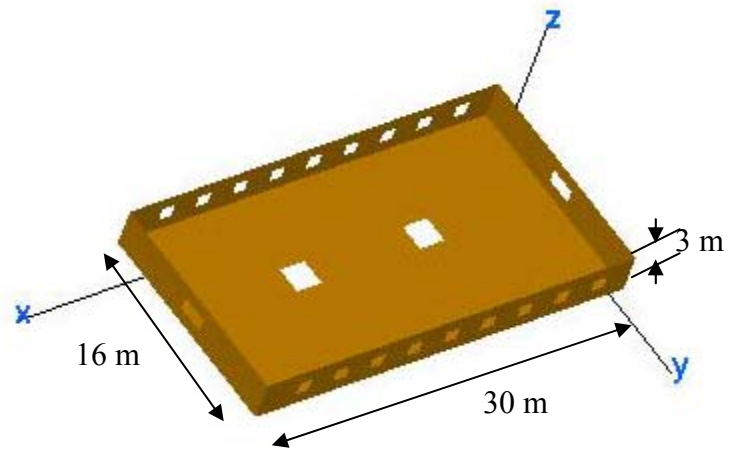


Figure 18. Model of the first-floor

The next step in the building process was to design the office spaces or hotel rooms inside the exterior walls. The interior walls are shown in Figure 19. Each room has a window and one door.

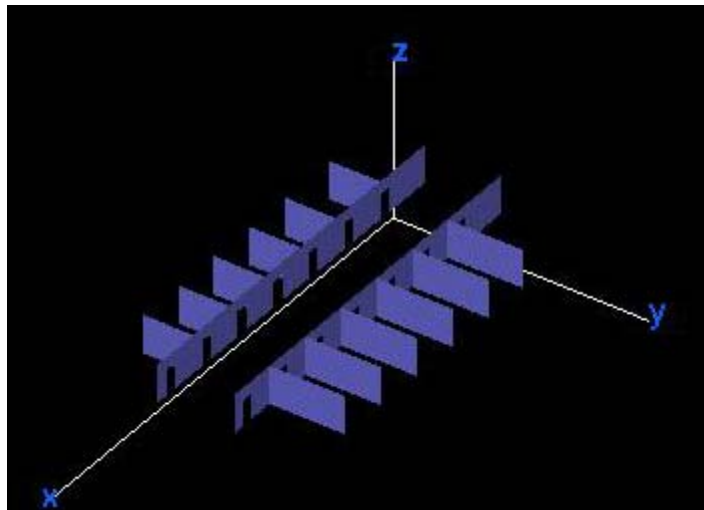


Figure 19. Walls inside the second-floor

The next phase of the building process was to design the spaces for the elevators. The elevators are designed to have four identical walls, or surfaces. The material used for the spaces is assigned a value of $icoat = 4$ because it usually has characteristics different from the other walls.

The model is designed with 11 upper floors, in addition to the lobby, necessitating making 11 copies of the basic floor. The final step was to combine all the resulting files using **Cifer** to get the complete model. Figure 20 shows the final model (where the roof was removed for the purpose to show the interior detail), with all eleven floors and a lobby. Each material (based on *icoat* values) has a different color in the figure to allow for better visualization the entire model.

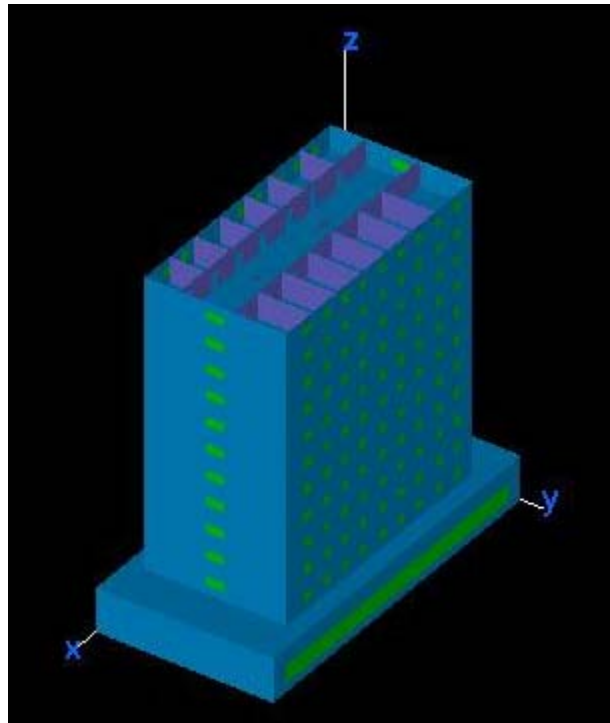


Figure 20. Completed model of the twelve story high rise (roof removed to show interior detail)

2. Extracting the Edges

For accurate simulation results, it is necessary to include edge diffraction in the calculation. Therefore, the diffracting edges must be specified in the **Urbana** input file. **Cifer** is capable of extracting edges from the surfaces, however, some corrections must be made manually, removing all non-diffracting edges. All resulting *edge* files are added together in order to obtain a total *edge* file for the model, similar to that shown in the Figure 21.

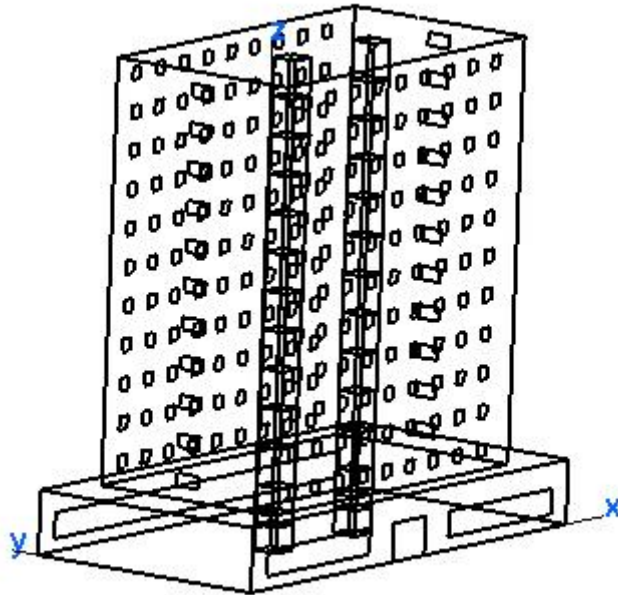


Figure 21. Edges of the high-rise model

C. RAY TRACING

Urbana calculates the scattered fields using one of several internal high frequency techniques. They include physical optics (PO), the physical theory of diffraction (PTD), geometrical optics (GO) and the geometrical theory of diffraction (GTD). In all cases, GO and GTD have been selected because they give adequate accuracy and require less computational time and computer memory than the other methods. Collectively these two methods are referred to as ray tracing, or microwave optics. The two ray techniques are illustrated in Figure 22.

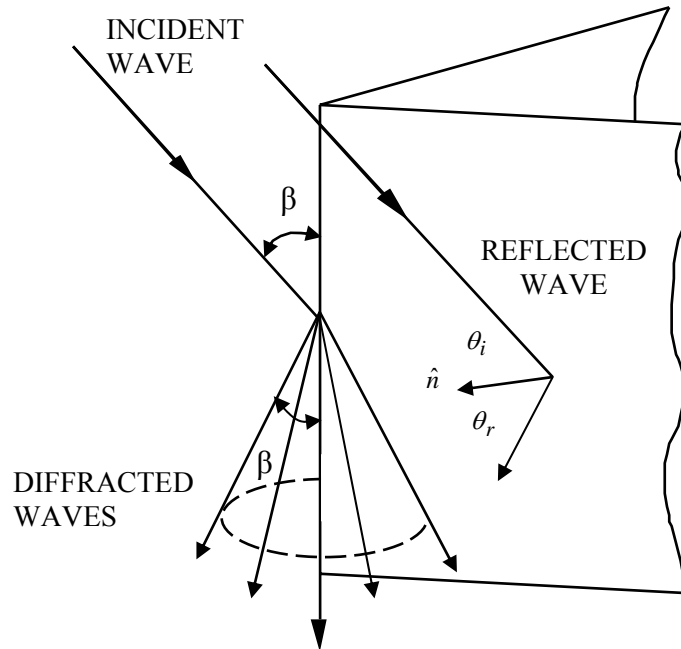


Figure 22. Example of reflected and diffracted rays

1. Geometrical Optics

Geometrical optics, refers to the classical theory of ray tracing used in the design and analysis of mirrors and lenses at optical frequencies. The main postulates of GO are as follows [12]:

- Waves are everywhere in locally plane,
- The wave direction is specified by the normal equiphase surface,
- Rays travel in straight lines,
- Polarization is constant along a ray, and
- Power in a flux tube is conserved.

The behavior of waves at interfaces is given by Snell's law, and the Fresnel reflection and transmission coefficients [12].

2. Geometrical Theory of Diffraction

The geometrical theory of diffraction was developed to improve on the GO approximation by adding edge-diffracted fields. Such diffracted rays operate as a secondary source of energy. The total field at a point in space is the sum of all reflected, direct, and diffracted fields arriving at that point. Formulas are available to compute the diffraction

from an edge [12]. The diffracted field is linearly related to the incident field at the diffraction point by a diffraction coefficient. The diffraction coefficient is dependent upon the angle of incidence onto the edge, the incident polarization, the wedge angle of the surfaces forming the edge, and the type of material. The diffracted ray trajectory lies on the surface of cone, which has a half-angle equal to the angle of incidence of the wave with the edges (β in Figure 22).

3. Ray Tracing

Urbana has the capability to save and plot rays that reflect from an object. This process is referred to as “shooting rays.” The ray tracing function in **Urbana** allows the shooting of rays so that the paths can be plotted in **Xcell**. A sample plot is shown in Figure 23.

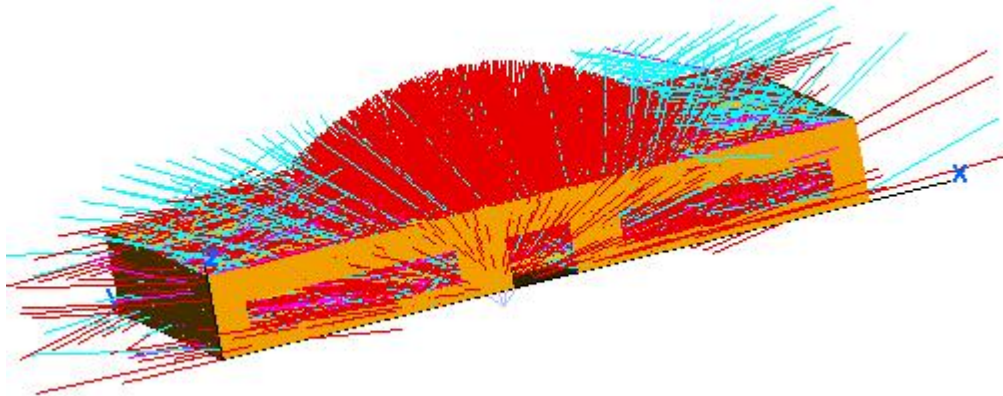


Figure 23. Example of shooting rays for the first floor

The different colors of rays describe four different levels of signal strength, starting with the highest (red) and successively weaker (violet, yellow and blue, respectively). The material for the walls was concrete, and the covering for the floor was PEC. The rays were launched in 2° angular increments and 10 bounces were allowed. Of course, most rays exited the model after only 2 or 3 bounces because of the open ceiling.

This chapter described the process of building the model and the different software used to accomplish a simulation. The next chapter will describe the principle concerns of simulating an indoor environment and show results for the single floor and high-rise building.

THIS PAGE INTENTIONALLY LEFT BLANK

IV. URBANA SIMULATION AND RESULTS

In the last chapter we described the process of building the physical model of the propagation environment using **Rhino**. When this step is completed, the file is saved in *iges* format and then imported to **Cifer** and converted to a *facet* file, which is the format read by **Urbana**. In this chapter the various simulations and their results are described. The first step was to study a single floor, looking at the effect of window and door locations and different materials. Next, the floors were stacked and a lobby added to form the high-rise office building or hotel. The propagation from floor to floor was analyzed by locating the transmitter on one floor and the observation points on another.

A. OBSERVATION POINTS FILE

Urbana computes the components of the electric field at observation points provided in a text file with their three-dimensional coordinates (x, y, z) . The observation plane is a set of points where the electromagnetic field is computed. The **Urbana** suite of programs includes one program for the purpose of observation point generation, but the points are restricted to planes parallel to the x - y plane. For more flexibility, a **Matlab** script was created to generate points in any arbitrary plane in space, and save them to a text file. For calculation of the field in horizontal or vertical planes, a step of 0.5 m between points was used over the observation plane that is 100 m by 50 m.

B. PROPAGATION ON A SINGLE FLOOR

The indoor environment is characterized by its dynamic changes due to people and their movements, and the varying of permittivity and permeability of walls and furniture. To develop an approximation of the real propagation in such an environment, a time snapshot (i.e., a fixed picture of the environment) is used to obtain the physical model. The first series of simulations examine the propagation characteristics of a single floor. The arrangement of rooms is indicated by the edges (dark lines) in Figure 24. This floor plan was reproduced and stacked to form the floors of high-rise building. All floors were identical, except for the ground floor, as described in the last chapter.

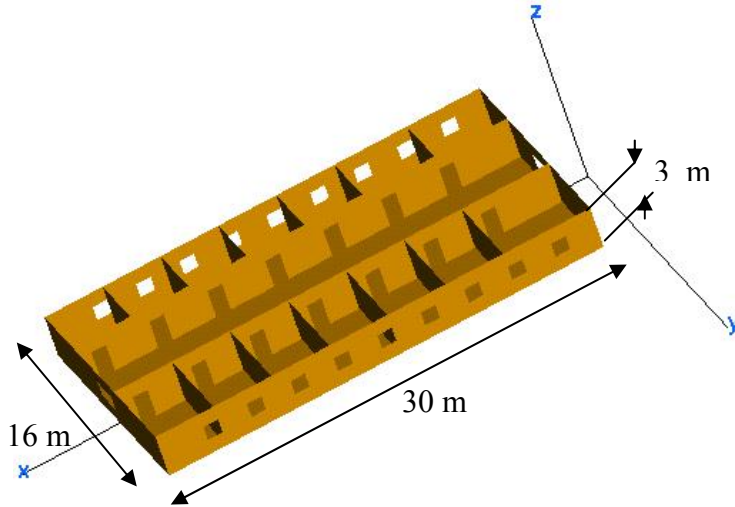


Figure 24. Model of a single floor

1. Open Doors and Windows

To begin with, the walls are considered PEC and the doors and windows to be open. Also, all of the cases used a transmitter power of 1 W. The input data for **Urbana** is shown in Table 2.

Input parameter	Value
Urbana input file:	floor2_simulation1.ur_input.
Input facet file:	floor2_simualtion1.facet
Length unit:	meters
Frequency:	2.4 GHz
Power level:	1 W
Antenna types:	Vertical Dipole
Antenna coordinates:	20,10,2
Observation point file:	obs_floor2.text
Computation methods:	GO
Edge diffraction option:	Yes
Edge file:	floor2_simulation1.edge
Ray spacing:	2.0

Table 2. Input data for the single floor simulation, with open doors and windows

When we run **Urbana**, an output file with the extension “.*field*” is generated. It contains a table of electric field components at each observation point. By using the *f2f* program, the data is converted to signal contours that can be visualized using **Xcell**. Taking the above simulation as example, the **Urbana** input is “floor2_simulation1.ur_input” and the generated output file is “floor2_simulation1.field”. Now the *f2f* script is used to convert the *field* file data to signal contour with a *facet* format. The responses to the *f2f* input are listed in Table 3.

Input parameter	Value
Plot magnitude:	4-Magnitude of Etot
Number of field files:	1
Filed file #1:	floor2_simulation1.field
Histogram interval:	10
Clip minimum:	-200 dBm
Clip maximum:	24.2 dBm
Range minimum:	-70 dBm
Range maximum:	24.2 dBm
Number of level:	25
Coding code of 1 st level:	1
Output file name:	floor2_simulation1.out.facet
Side of sample:	0.5
Shift data in z:	y
Offset data:	0

Table 3. Responses to input when running *f2f* for the simulation in Table 2

Figure 25 displays the superposition of the edge file and the signal contours using **Xcell**. The color scale present at the right of this figure gives the color-coded power level. The red color shows the maximum value and the blue color is the minimum. The minimum power is set to the value of -70 dBm, because this value is the typical sensitivity of current commercially available receivers.

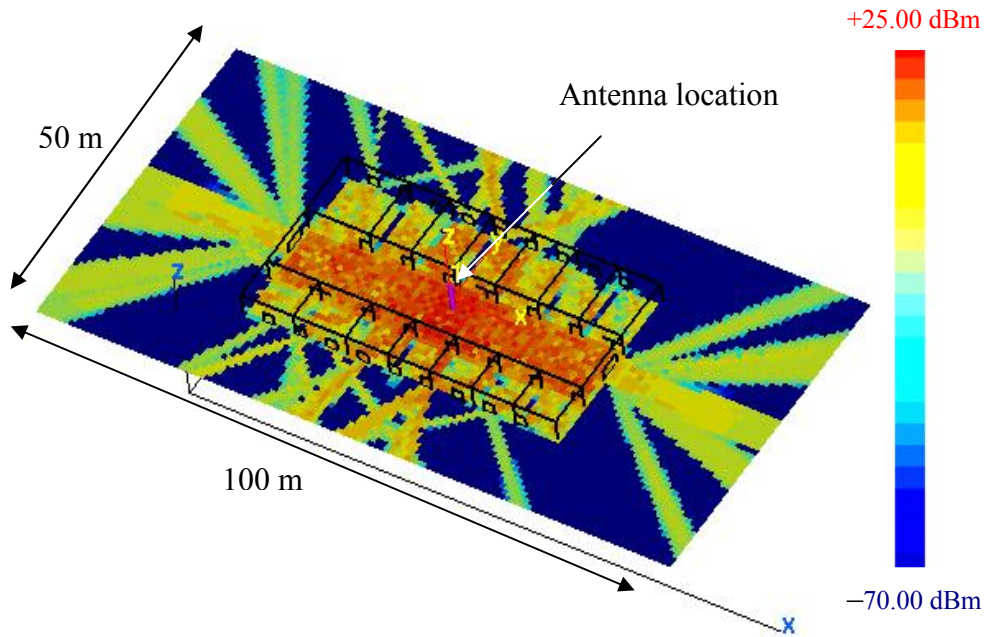


Figure 25. Signal contour for all PEC surfaces with open doors and windows

2. Closed Doors and Open Elevator Shafts

Next we modified the model so that the interior doors were closed. These doors are considered PEC, as are the walls ($icoat = 0$). Two elevator openings were added as shown in Figure 26. The new parameters for the **Urbana** input file are shown in Table 4. The corresponding *f2f* script to convert the *field* file to *facet* file is shown in Table 5. The resulting signal contours are shown in Figure 27.

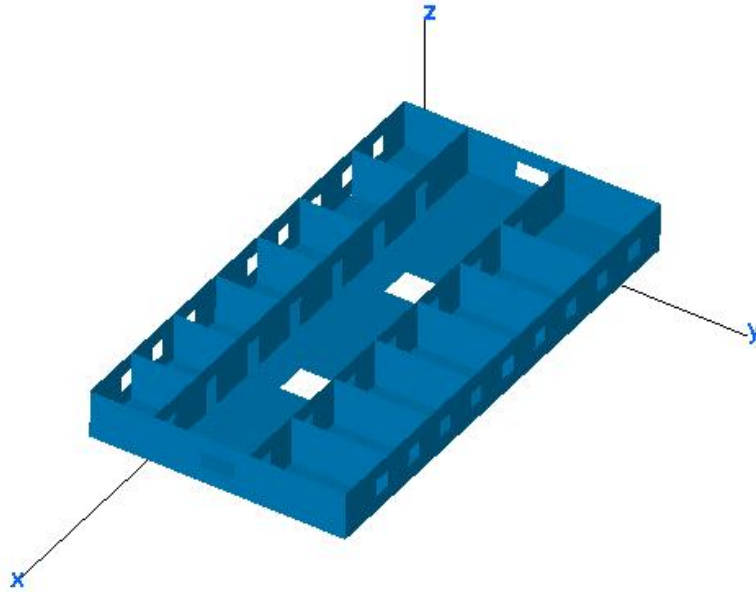


Figure 26. Model of single floor with elevator openings

Input parameter	Value
Urbana input file:	floor2_simulation2.ur_input.
Input facet file:	floor2_simualtion2.facet
Length unit:	meters
Frequency:	2.4 GHz
Power level:	1 W
Antenna types:	Vertical Dipole
Antenna coordinates:	20,10,2
Observation point file:	obs_floor2.text
Computation methods:	GO
Edge diffraction option:	Yes
Edge file:	floor2_simulation2.edge
Ray spacing:	2.0
Ray bounces:	5
Material options:	<i>icoat</i> = 0 (PEC)

Table 4. Input data for the single floor simulation, with closed doors

Input parameter	Value
Plot magnitude:	4-Magnitude of Etot
Number of field files:	1
Filed file #1:	floor2_simulation2.field
Histogram interval:	10
Clip minimum:	-200 dBm
Clip maximum:	23.5 dBm
Range minimum:	-70 dBm
Range maximum:	23.5 dBm
Number of level:	25
Coding code of 1 st level:	1
Output file name:	floor2_simulation2out.facet
Side of sample:	0.5
Shift data in z:	y
Offset data:	0

Table 5. Responses to input when running $f2f$ for simulation in Table 4

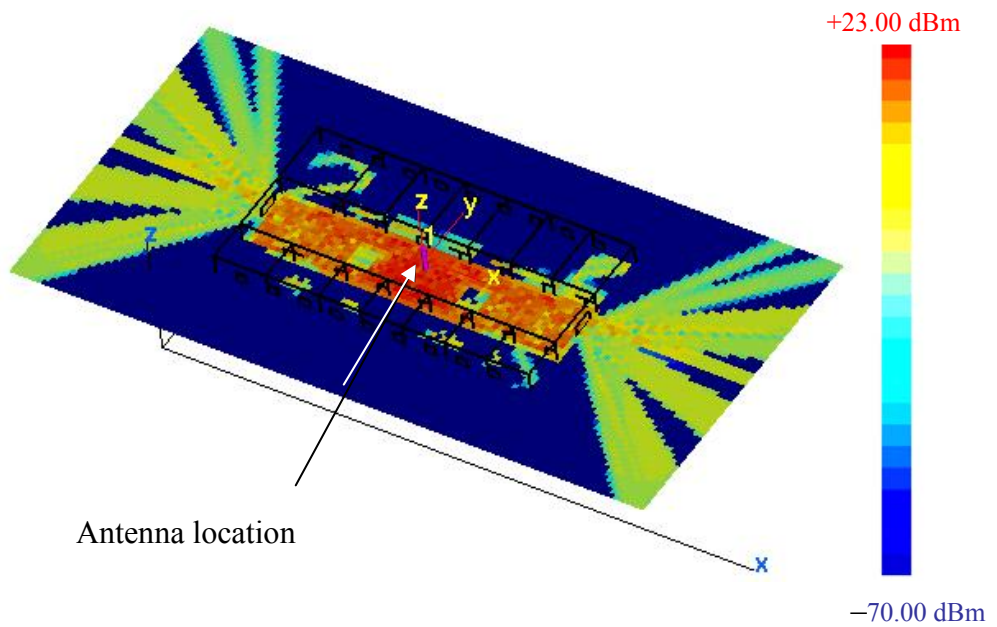


Figure 27. Signal levels for the case all PEC surfaces with interior doors closed

The maximum power level is near the location of the antenna, with a value of 23 dBm. Most of the energy is confined to the walkway or common area. The signal levels inside of the rooms are very low for the closed door model, as expected. If the rooms were tightly sealed with PEC doors there should be no signals inside the rooms. However, the edges in the model are not exactly coincident, and therefore some diffraction may occur. There is also some diffraction over the top edges of the walls since there is no ceiling present.

3. High-Fidelity Model with Open Doors

For the next simulation, elevator shaft enclosures were added, and more realistic materials used. This is referred to the “high-fidelity” model. Figure 28 shows the floor plan, and the materials are color coded according to their *icoat* values. Table 6 lists the *icoat* values and the corresponding materials. The length of the floor is 30 m, the width 16 m, and the height 3 m.

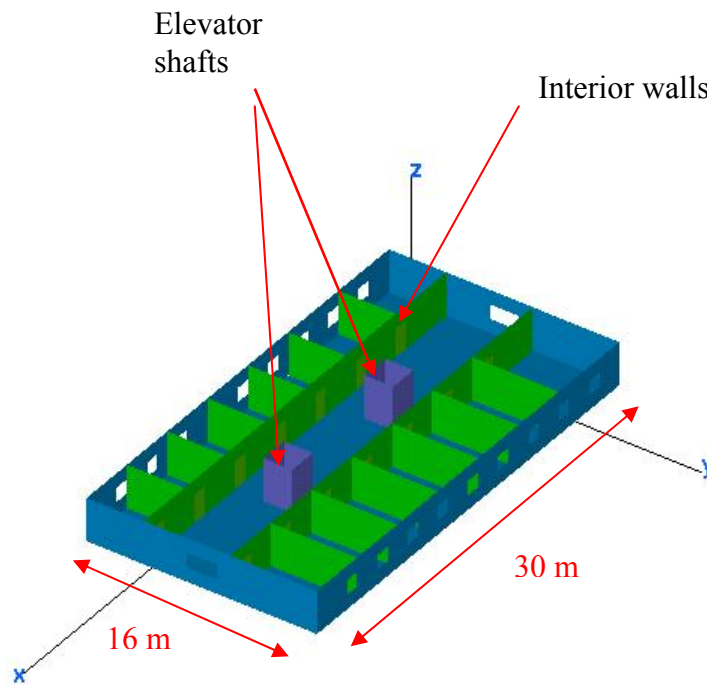


Figure 28. Floor layout with elevator shafts

Component	<i>icoat</i>	Material	Complex permittivity	Complex permeability	Thickness (meters)	Resistivity (ohms)
Exterior walls	1	Concrete	$10.1 + j0.50$	1	0.3	10^{30}
Interior walls	2	Concrete	$10.1 + j0.50$	1	0.1	10^{30}
Doors	3	Wood	$3.0 + j0.67$	1	0.05	10^{30}
Windows	4	Glass	$6.0 + j0$	1	0.01	10^{30}
Elevator rooms	2	Concrete	$10.1 + j0.50$	1	0.1	10^{30}

Table 6. Material specifications for the high-fidelity model

The first simulation using the high-fidelity model had open interior doors. The **Urbana** input file parameters are listed in Table 7. The material types are defined at the end of the input file (values 1 through 4 in Table 7). The *icoat* values are a shorthand notation for a complete description of the material based on its permittivity, permeability, resistivity and physical configuration (e.g., layers with material backing).

Input parameter	Value
Urbana input file:	floor2_simulation3.ur_input.
Input facet file:	floor2_simualtion3.facet
Length unit:	meters
Frequency:	2.4 GHz
Power level:	1 W
Antenna types:	Vertical Dipole
Antenna coordinates:	20,10,2
Observation point file:	obs_floor2.text
Computation methods:	GO
Edge diffraction option:	Yes
Edge file:	floor2_simulation3.edge
Material options:	<i>icoat</i> = 1,2,3 and 4

Table 7. Input parameter for the high-fidelity model

Table 8 shows the input to the *f2f* script, to convert the field file into a *facet* file. The signal contours are shown in Figure 29.

Input parameter	Value
Plot magnitude:	4-Magnitude of Etot
Number of field files:	1
Filed file #1:	floor2_simulation3.field
Histogram interval:	10
Clip minimum:	-200 dBm
Clip maximum:	20.88 dBm
Range minimum:	-70 dBm
Range maximum:	20.88 dBm
Number of level:	25
Coding code of 1 st level:	1
Output file name:	floor2_simulation3out.facet
Side of sample:	0.5
Shift data in z:	y

Table 8. Inputs for running *f2f* program for the simulation in Table 7

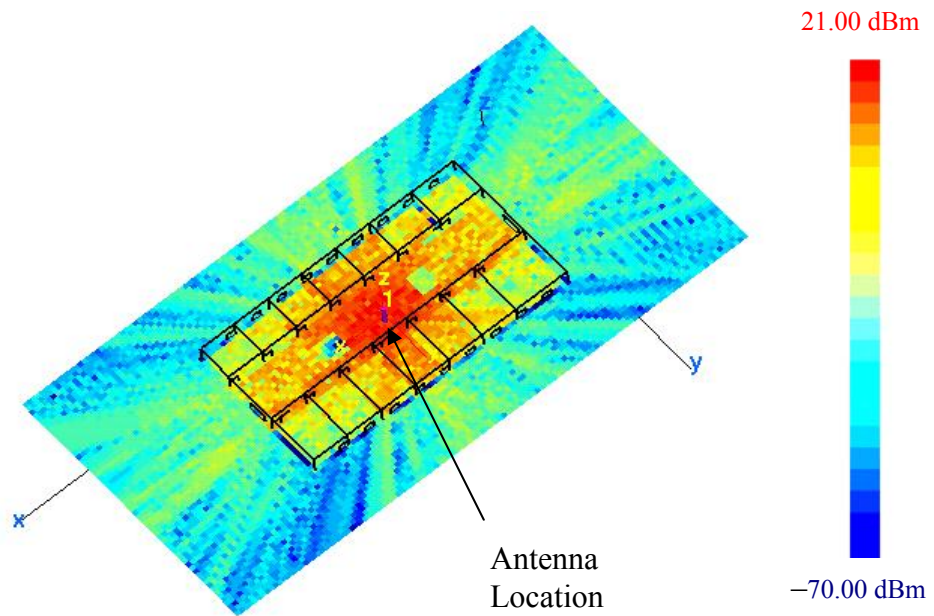


Figure 29. Signal levels for the high-fidelity model with open doors

4. High-Fidelity Model with Close Doors

The next simulation was for a closed door configuration. The doors were considered to be wood, with the parameters listed in Table 6. The **Urbana** input parameters are given in Table 9, and the *f2f* input responses are listed in Table 10.

Input parameter	Value
Urbana input file:	floor2_simulation4.ur_input.
Input facet file:	floor2_simualtion4.facet
Length unit:	meters
Frequency:	2.4 GHz
Power level:	1 W
Antenna types:	Vertical Dipole
Antenna coordinates:	20,10,2
Observation point file:	obs_floor2.text
Computation methods:	GO
Edge diffraction option:	Yes
Edge file:	floor2_simulation4.edge
Ray spacing:	2.0
Ray bounces:	5
Material options:	<i>icoat</i> = 1,2,3,4

Table 9. Input parameter for the high-fidelity model with closed doors

As expected, the signal level is strongest close to the antenna as seen in Figure 30. Since the doors are wood and the windows are glass (with the characteristics defined in Table 6), there is transmission into the offices on the floor, even when the doors are closed. Figures 29 and 30 show only slight difference in the power level due to the position of the doors.

Input parameter	Value
Plot magnitude:	4-Magnitude of Etot
Number of field files:	1
Filed file #1:	floor2_simulation4.field
Histogram interval:	10
Clip minimum:	-200 dBm
Clip maximum:	22.4 dBm
Range minimum:	-70 dBm
Range maximum:	22.4 dBm
Number of level:	25
Coding code of 1 st level:	1
Output file name:	floor2_simulation4out.facet
Side of sample:	0.5
Shift data in z:	y
Offset data:	0

Table 10. Inputs for running *f2f* program for the simulation in Table 9

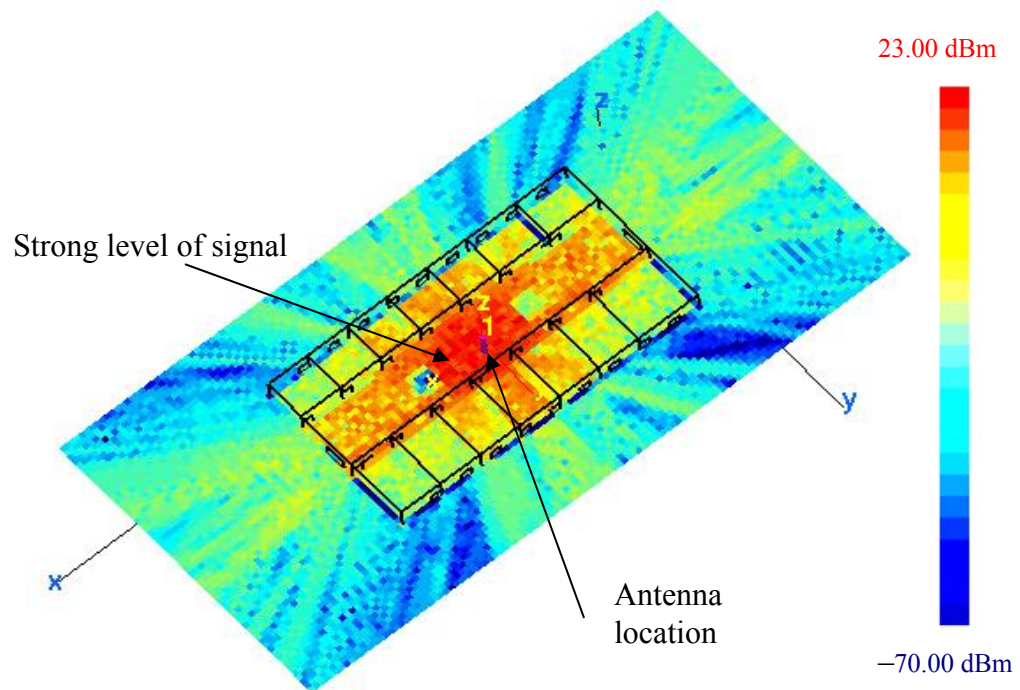


Figure 30. Signal contour for the high-fidelity model with closed doors

C. PROPAGATION BETWEEN FLOORS OF A HIGH-RISE BUILDING

1. Simulations of a PEC Building

Using **Rhino**, a high-rise building comprised of a lobby and eleven upper floors was designed. Floors two through twelve were exact duplicates of the single floor simulated in Section C. The first floor is a concourse or lobby area. The complete building model is shown in Figure 31. The details of building the model were discussed in Chapter III.

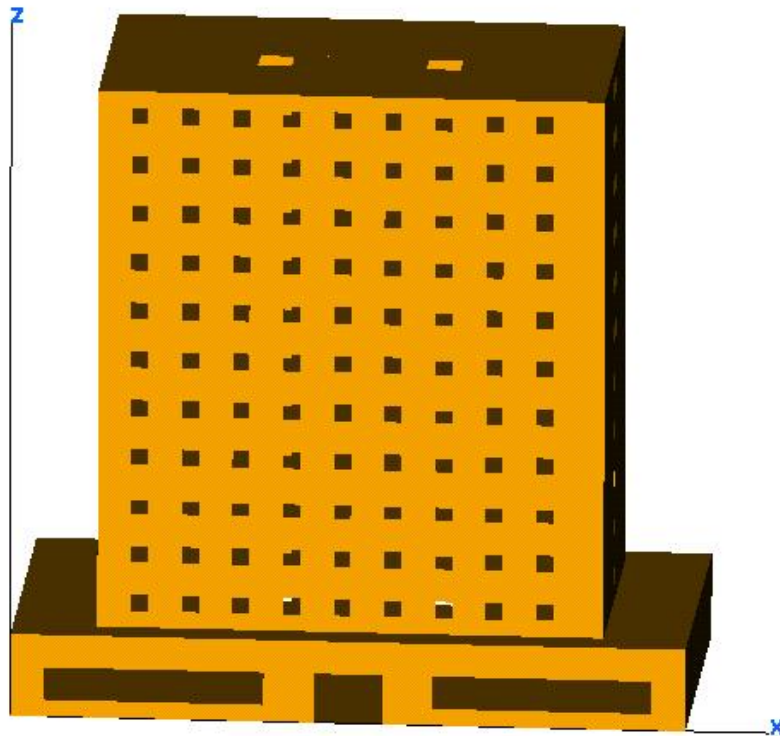


Figure 31. High-rise building model

The outside walls are PEC and all windows are open for the first simulation. The objective of this series of simulations was to examine the propagation between floors of the building. It was started by placing an antenna in the middle of the building on the 7th floor. The power transmitted by the antenna was 1 Watt. The observation points were placed on each floor, 1 meter above floor level. In this set of simulations the information

in the input file was the same, except for the change in the observation point file (according to the floor number). Table 11 lists the input parameters.

Input parameter	Value
Urbana input file:	modell_PEC#.ur_input.
Input facet file:	modell.facet
Length unit:	meters
Frequency:	2.4 GHz
Power level:	1 W
Antenna types:	Vertical Dipole
Antenna coordinates:	20,10,21
Observation point file:	obs_floor#.text
Computation methods:	GO
Edge diffraction option:	Yes
Edge file:	modell.edge
Ray spacing:	2.0
Ray bounces:	5
Material options:	<i>icoat</i> = 0 (PEC)

Table 11. **Urbana** input parameters

There are a total of 12 simulations in this series. For each output *field* file the *f2f* script must be run. Table 12 lists the responses, which are identical for all twelve cases, except for the observation point file name. The signal contours are shown in Figures 32 through 43 for the PEC building with open windows.

Input parameter	Value
Plot magnitude:	4-Magnitude of Etot
Number of field files:	1
Filed file #1:	modell1_PEC#.field
Histogram interval:	10
Clip minimum:	-200 dBm
Clip maximum:	22.4 dBm
Range minimum:	-70 dBm
Range maximum:	22.4 dBm
Number of level:	25
Coding code of 1 st level:	1
Output file name:	modell1_PEC#_out.facet
Side of sample:	0.5
Shift data in z:	y

Table 12. Inputs for running *f2f* program for the simulation in Table 11

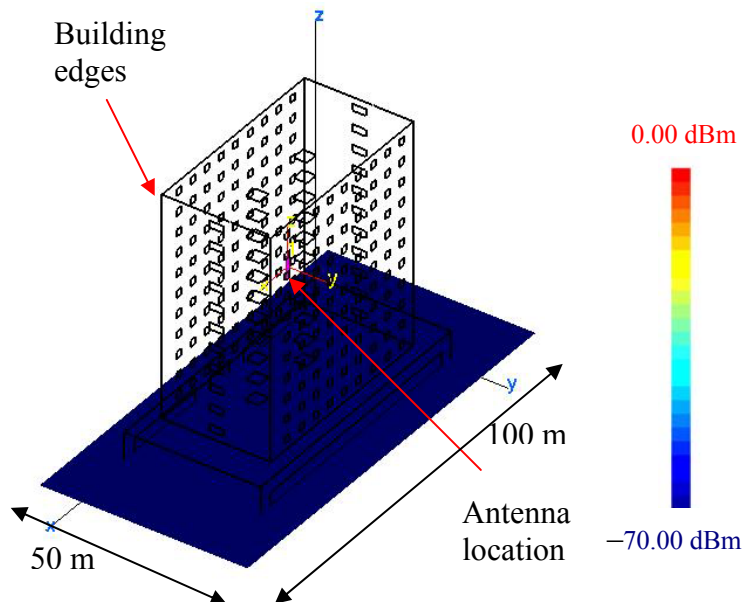


Figure 32. Signal contour for the first floor lobby (PEC building, open windows transmitter on the seventh floor)

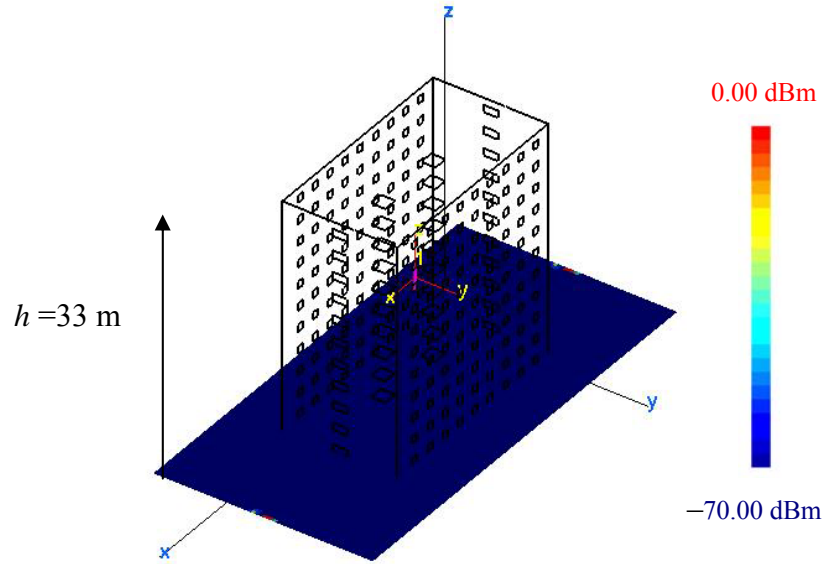


Figure 33. Signal contour for the second floor (PEC building, open windows transmitter on the seventh floor)

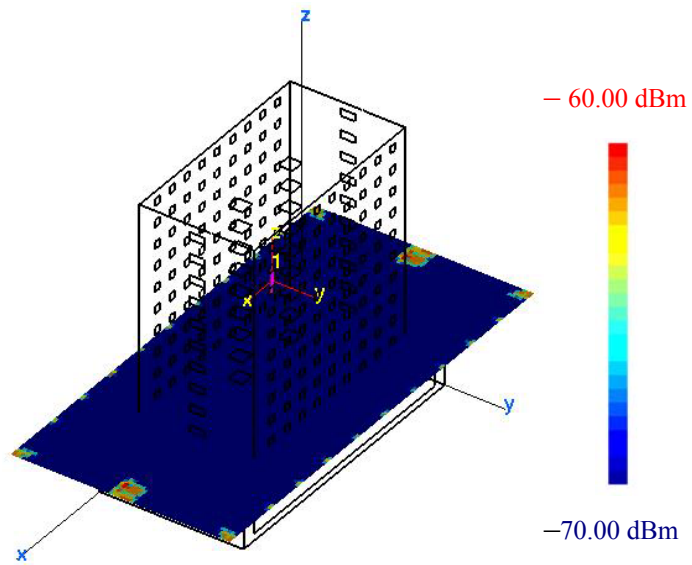


Figure 34. Signal contour for the third floor (PEC building, open windows transmitter on the seventh floor)

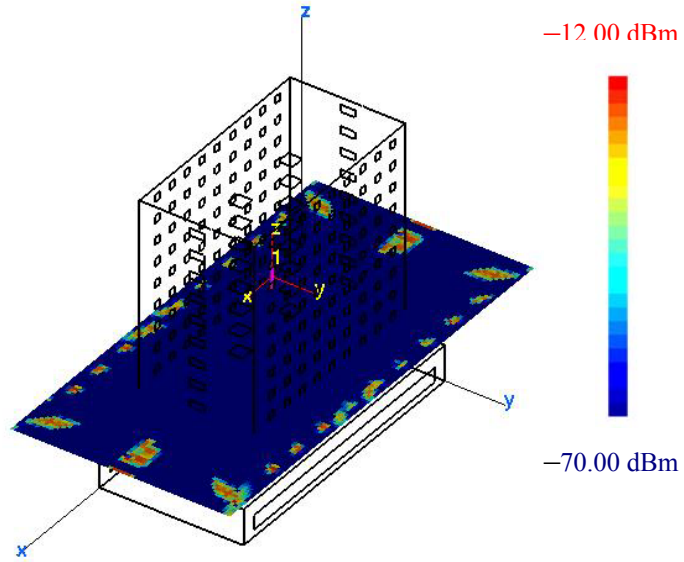


Figure 35. Signal contour for the fourth floor (PEC building, open windows transmitter on the seventh floor)

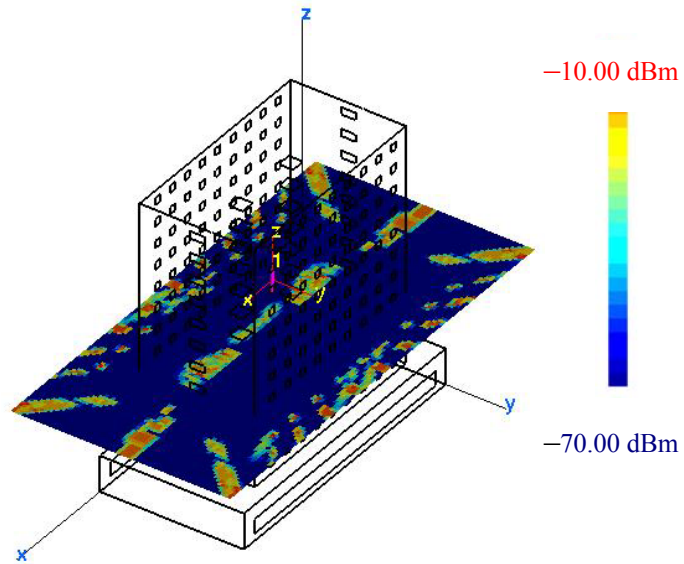


Figure 36. Signal contour for the fifth floor (PEC building, open windows transmitter on the seventh floor)

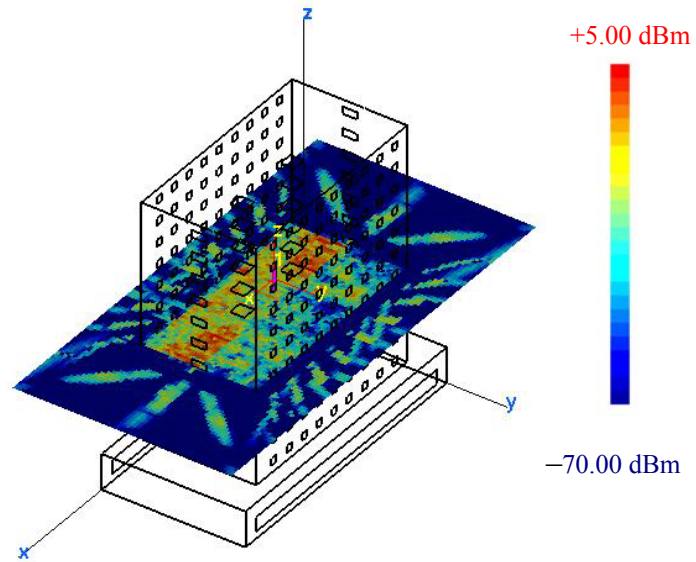


Figure 37. Signal contour for the sixth floor (PEC building, open windows transmitter on the seventh floor)

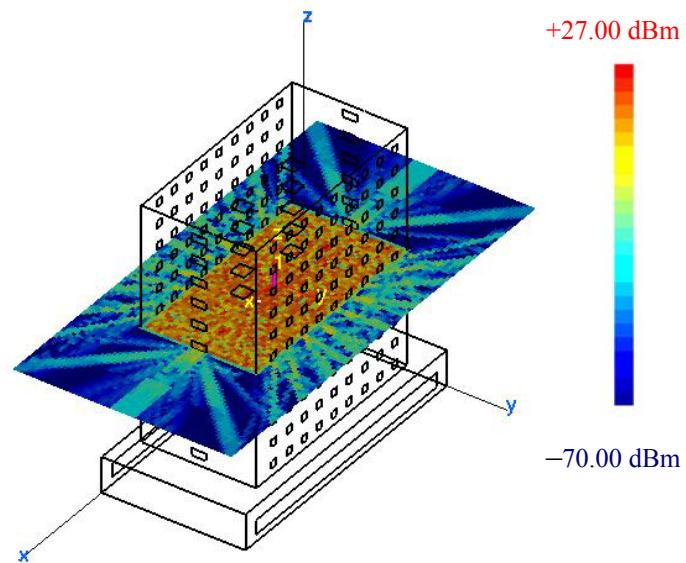


Figure 38. Signal contour for the seventh floor (PEC building, open windows transmitter on the seventh floor)

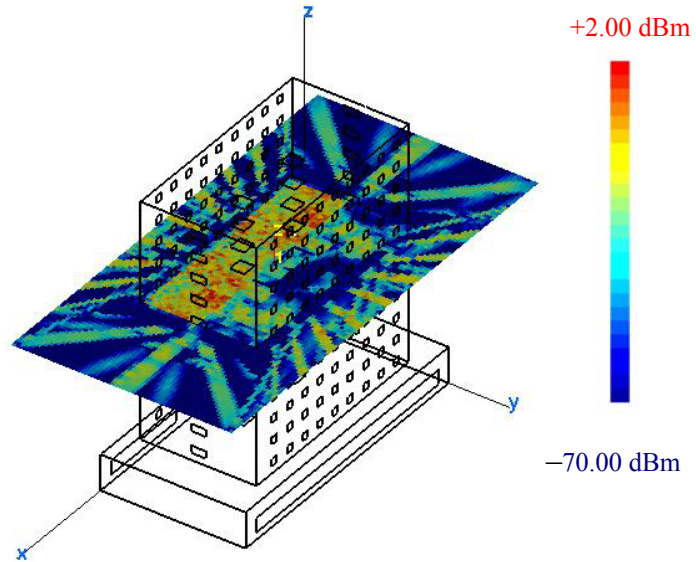


Figure 39. Signal contour for the eighth floor (PEC building, open windows transmitter on the seventh floor)

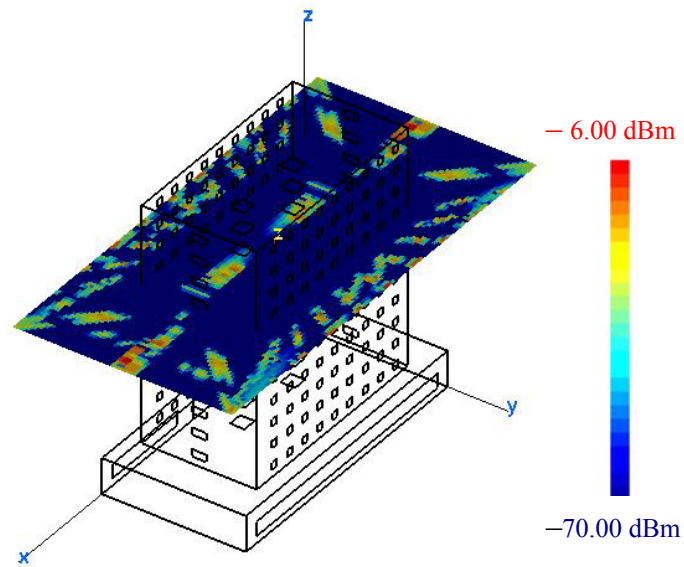


Figure 40. Signal contour for the ninth floor (PEC building, open windows transmitter on the seventh floor)

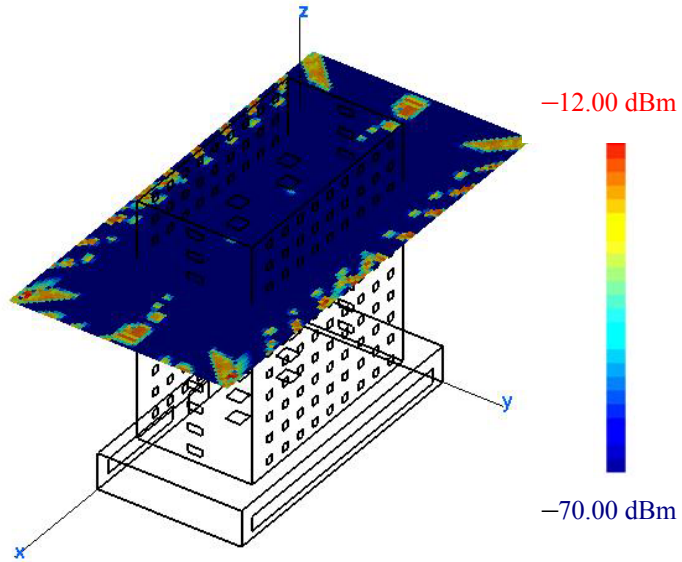


Figure 41. Signal contour for the tenth floor (PEC building, open windows transmitter on the seventh floor)

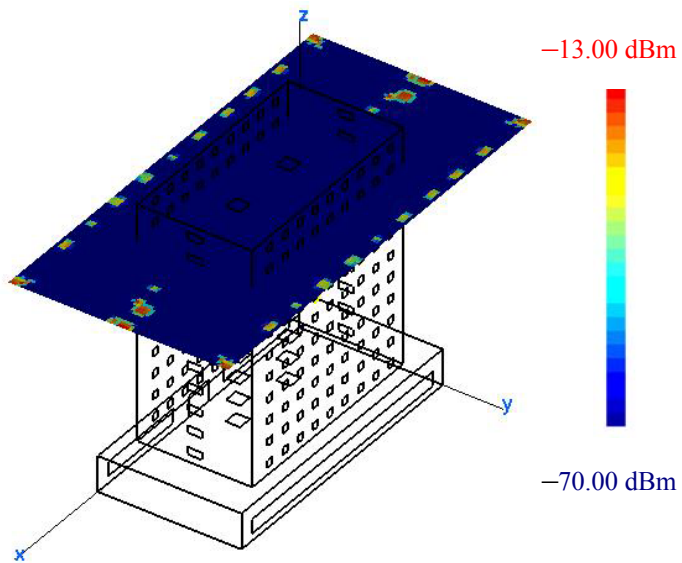


Figure 42. Signal contour for the eleventh floor (PEC building, open windows transmitter on the seventh floor)

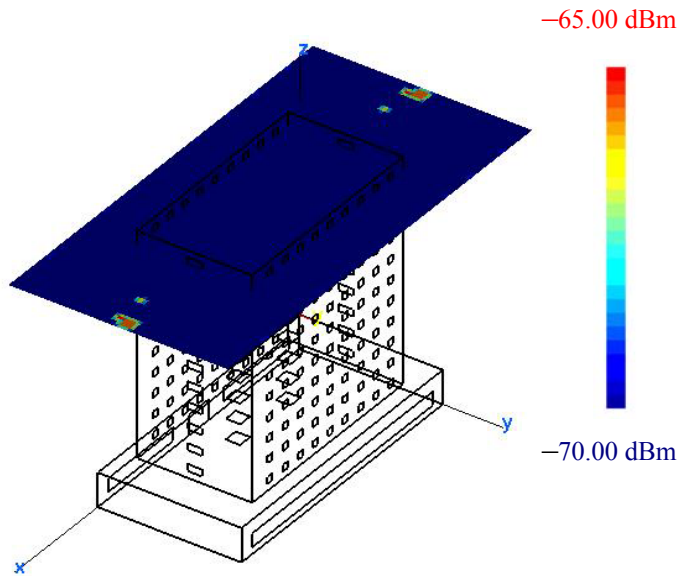


Figure 43. Signal contour for the twelfth floor (PEC building, open windows transmitter on the seventh floor)

A comparison of the figures shows that little or none of the signal reaches the fourth floor or lower. The noticeable signals outside of the building are due to diffraction from the window edges. The first appearance of strong signal occurs on the fifth floor (two floors below the antenna). As expected the maximum signal levels occur on the same floor as the antenna (Figure 38). There are areas of significant signal on the eighth through tenth floors as well. Some of these areas are near the elevator shafts, which were left open for the simulation. The chart in Figure 44 shows the maximum signal levels on each floor of the building.

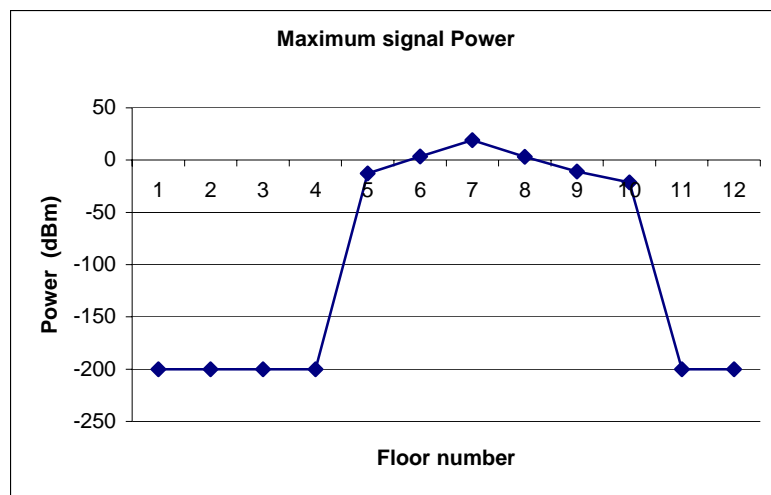


Figure 44. Maximum signal level on each floor inside the building (PEC high-rise building, open windows and the transmitter on the seventh floor)

2. Simulation Using a High-Fidelity Building Model

The second set of simulations with the high-rise building used different materials for each component of the building. The characteristic of each material was defined in Table 6. The main change in the **Urbana** input file was to switch from the option “ALL PEC” to “With Material,” and define the permittivity, permeability, thickness and resistivity of each *icoat* structure. The simulation was run for each floor to see the propagation from floor to floor. Figure 45 displays the high-rise building with realistic materials for each component, where each material is described by a different color.

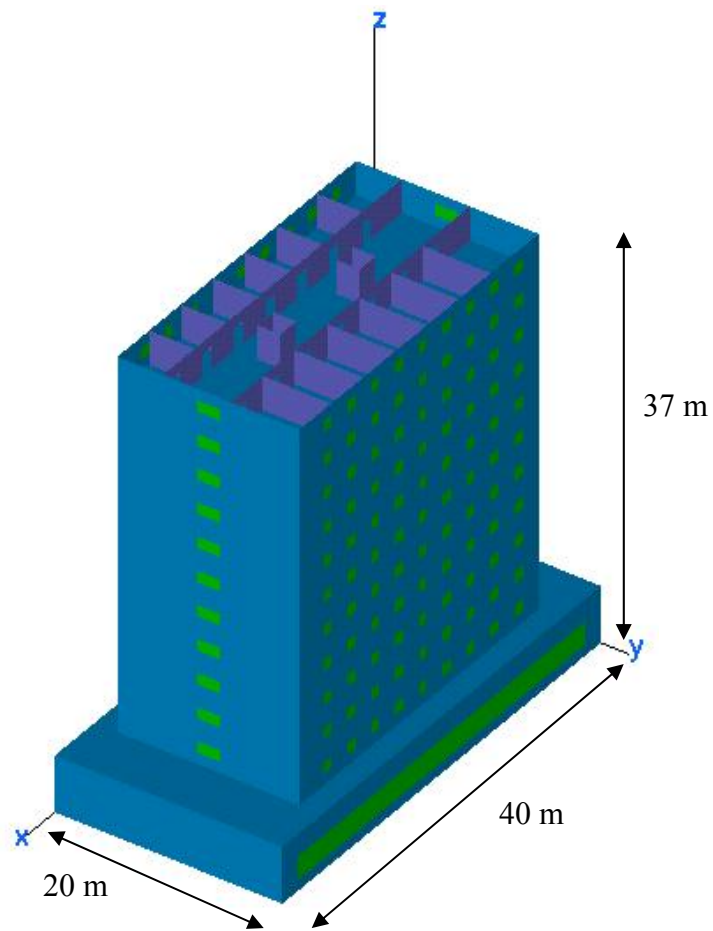


Figure 45. High-fidelity building

Table 13 gives the summary of the main input data for the **Urbana** file, followed by the inputs for running the *f2f* program in Table 14. The output results of the simulation of a high-fidelity model are shown in Figures 46 through 57.

Input parameter	Value
Urbana input file:	mode2_m#.ur_input.
Input facet file:	model2.facet
Length unit:	meters
Frequency:	2.4 GHz
Power level:	1 W
Antenna types:	Vertical Dipole
Antenna coordinates:	20,10,21
Observation point file:	obs_floor#.text
Computation methods:	GO
Edge diffraction option:	Yes
Edge file:	model2.edge
Ray spacing:	2.0
Ray bounces:	5
Material options:	<i>icoat</i> = 1,2,3,4

Table 13. **Urbana** input parameters for the high-fidelity building with realistic materials

Input parameter	Value
Plot magnitude:	4-Magnitude of Etot
Number of field files:	1
Filed file #1:	model2_m#.field
Histogram interval:	10
Clip minimum:	-200 dBm
Clip maximum:	17 dBm
Range minimum:	-70 dBm
Range maximum:	17 dBm
Number of level:	25
Coding code of 1 st level:	1
Output file name:	model2_m#_out.facet
Side of sample:	0.5
Shift data in z:	y
Offset data:	0

Table 14. Responses to input for running $f2f$ for the simulation in Table 13

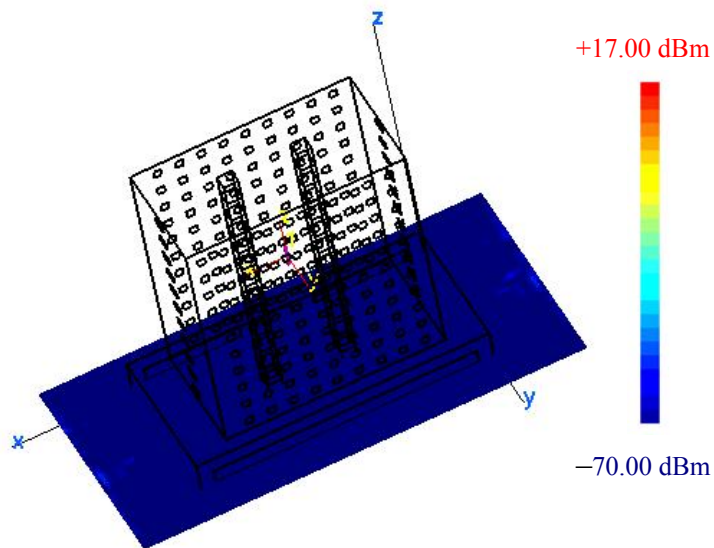


Figure 46. Signal contour for the first floor (high-fidelity building, open windows transmitter on the seventh floor)

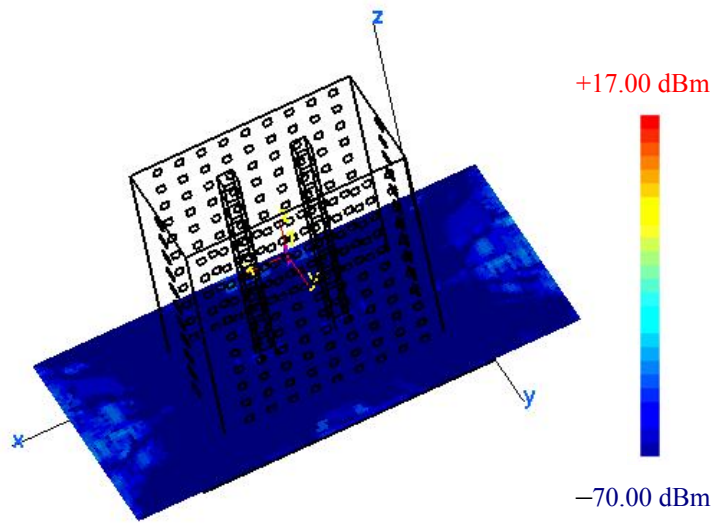


Figure 47. Signal contour for the second floor (high-fidelity building, open windows transmitter on the seventh floor)

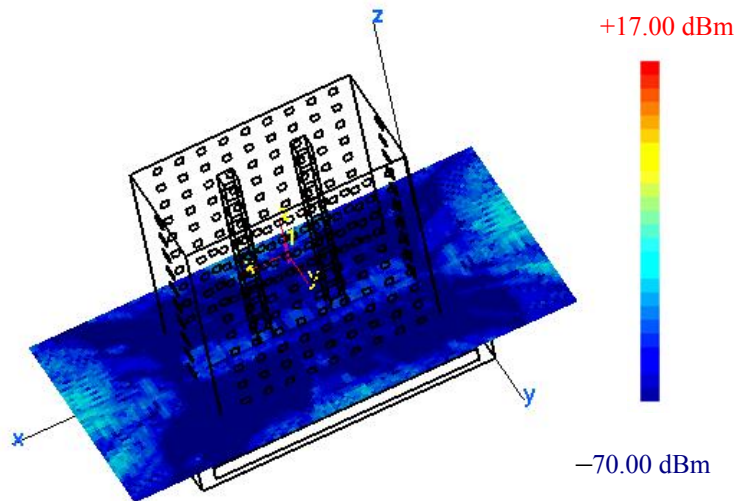


Figure 48. Signal contour for the third floor (high-fidelity building, open windows transmitter on the seventh floor)

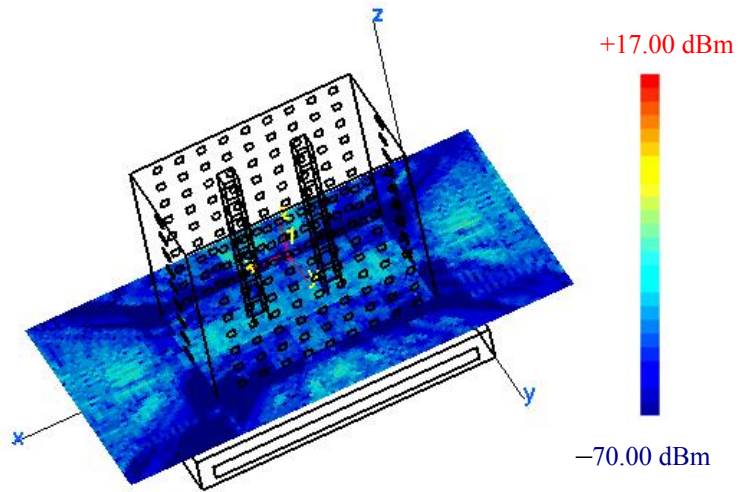


Figure 49. Signal contour for the fourth floor (high-fidelity building, open windows transmitter on the seventh floor)

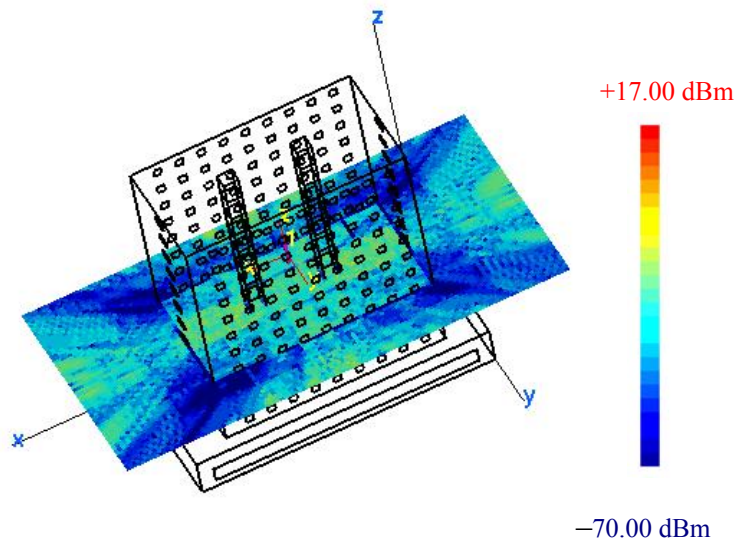


Figure 50. Signal contour for the fifth floor (high-fidelity building, open windows transmitter on the seventh floor)

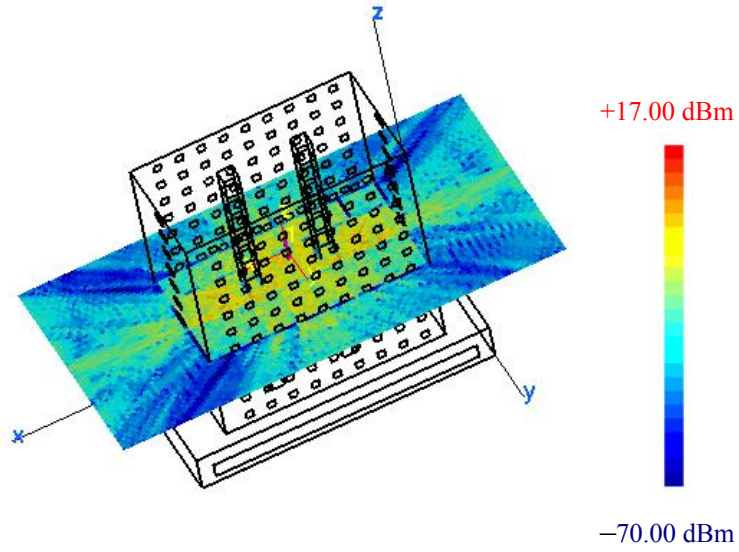


Figure 51. Signal contour for the sixth floor (high-fidelity building, open windows transmitter on the seventh floor)

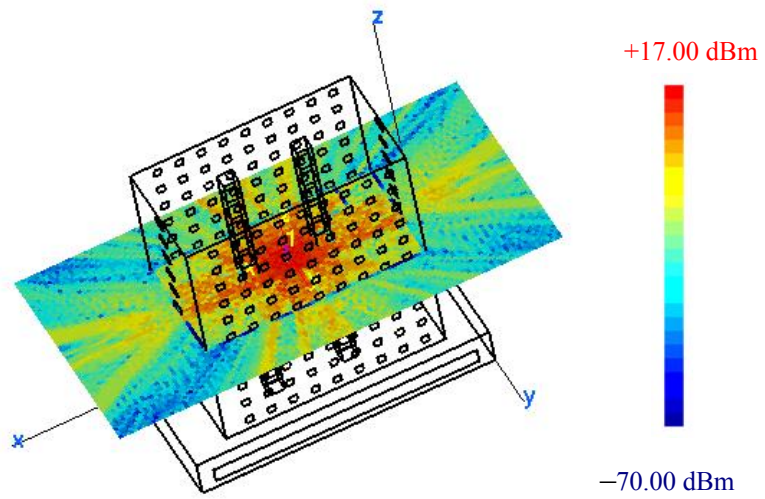


Figure 52. Signal contour for the seventh floor (high-fidelity building, open windows transmitter on the seventh floor)

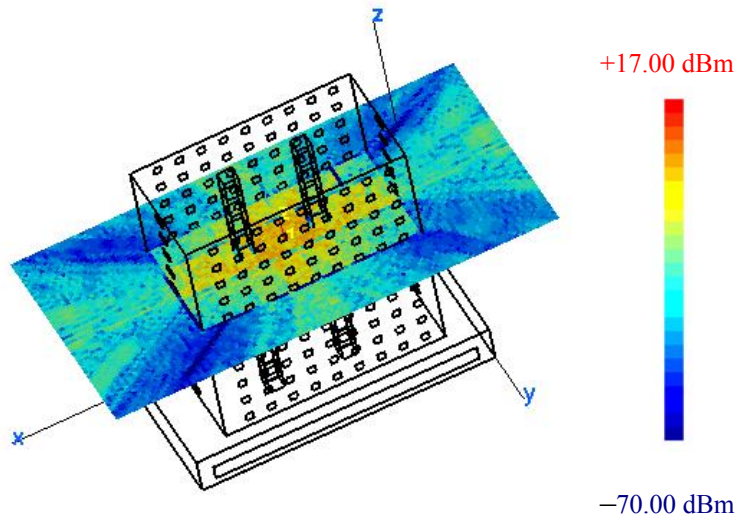


Figure 53. Signal contour for the eighth floor (high-fidelity building, open windows transmitter on the seventh floor)

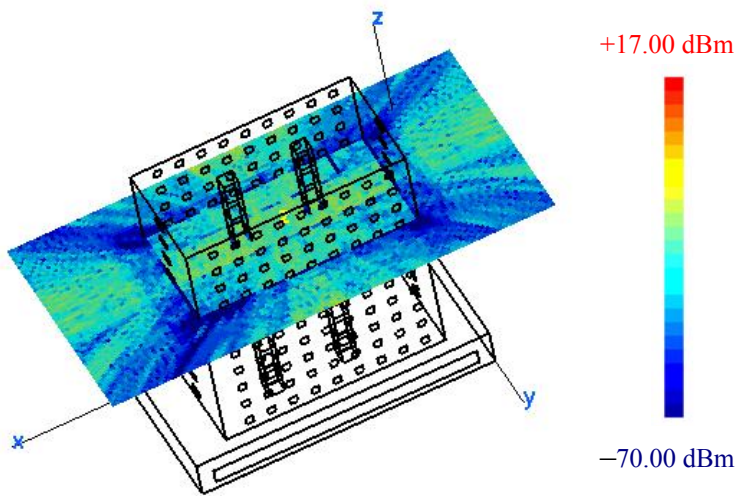


Figure 54. Signal contour for the ninth floor (high-fidelity building, open windows transmitter on the seventh floor)

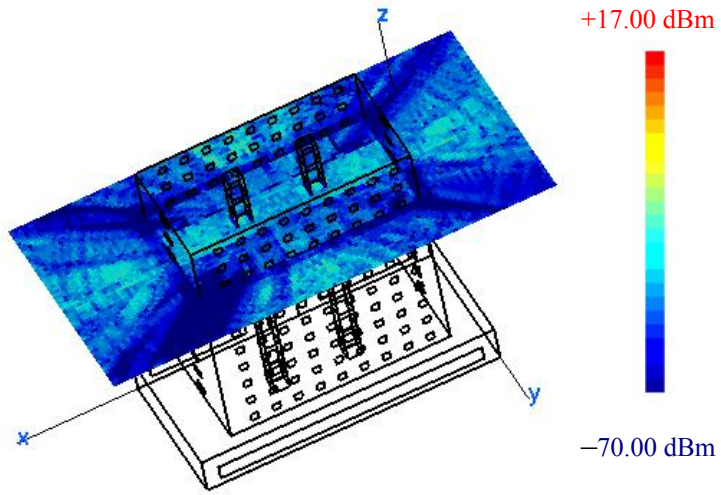


Figure 55. Signal contour for the tenth floor (high-fidelity building, open windows transmitter on the seventh floor)

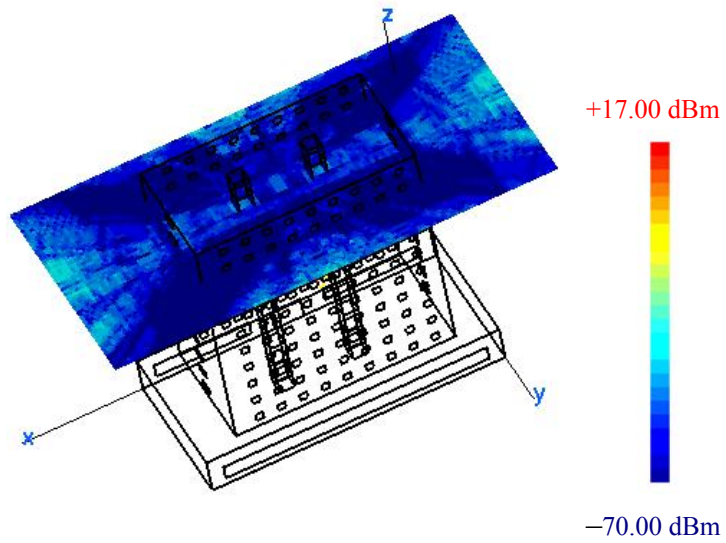


Figure 56. Signal contour for the eleventh floor (high-fidelity building, open windows transmitter on the seventh floor)

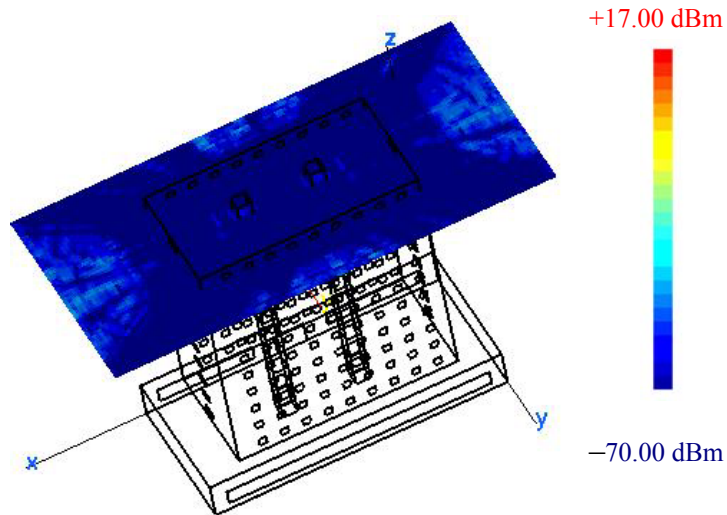


Figure 57. Signal contour for the twelfth floor (high-fidelity building, open windows transmitter on the seventh floor)

The results of the 12 simulations of the propagation inside of the high-rise model are summarized in Figure 58. The plot shows the maximum signal value on each floor. A **Matlab** program was generated to load the data from the *field* file and compute the signal level at each point of the observation plane inside the boundary of the building and then select the maximum value on each floor.

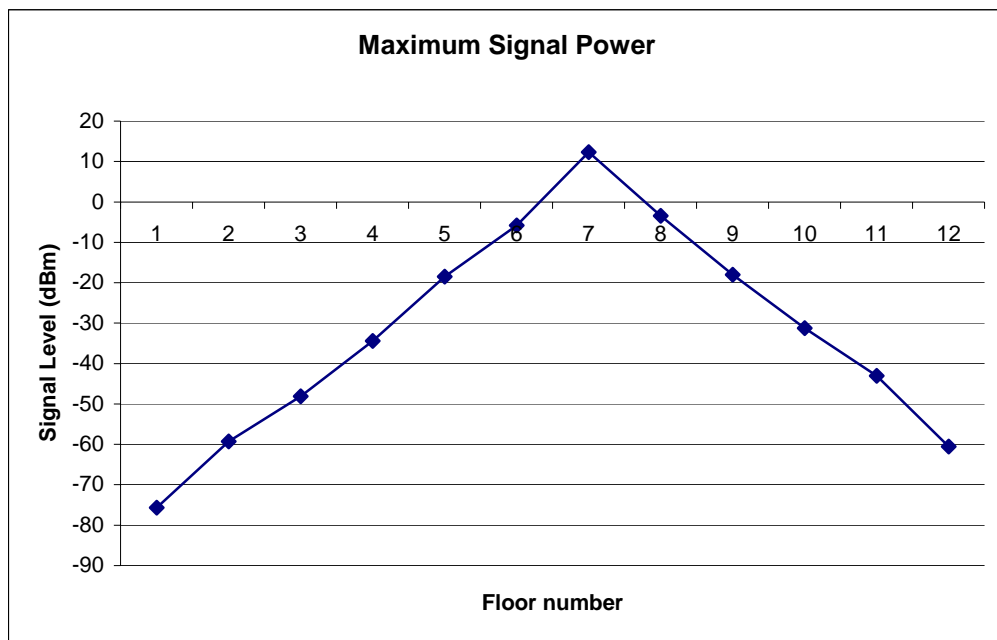


Figure 58. Maximum signal level on each floor inside the high-fidelity building (open windows and the transmitter on the seventh floor)

Another useful output is the estimate of loss between floors in high-rise building. The results of the loss between the maximum power level on each floor with the antenna on the first floor are summarized in Figure 59. The results show that the loss between floors is highest for the first few floors and then decreases for the higher floors. This trend was also found in [7].



Figure 59. Loss between floors for a high-fidelity building (antenna in the first floor, transmit power 1 W)

3. Transmit Power Level

The transmit power influences the signal level on each floor. Since all the parameters in the simulation model are linear, it is expected that the signal strength should vary directly with the transmit power. Figures 60 and 61 show the contour for transmitter powers of 1 W and 100 mW, respectively.

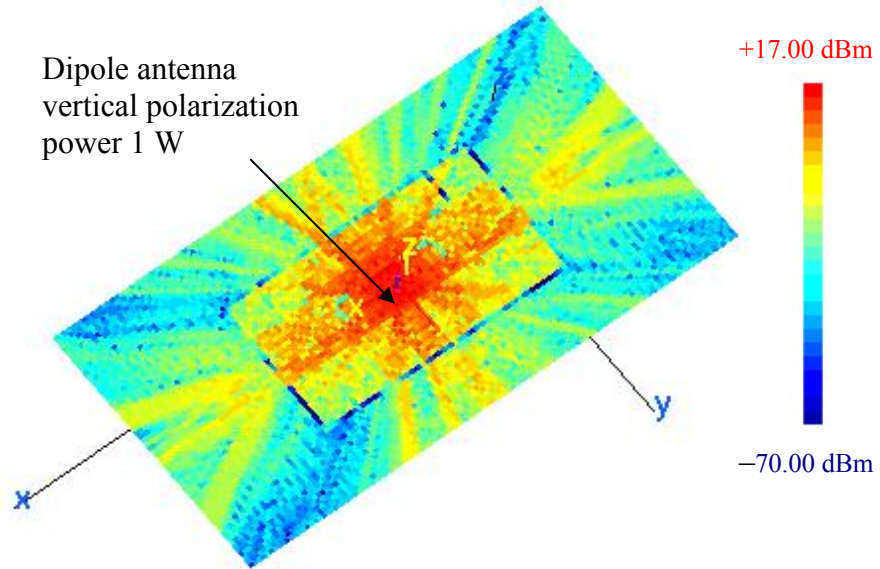


Figure 60. Signal contour for the seventh floor (1 W source power and antenna on the seventh floor)

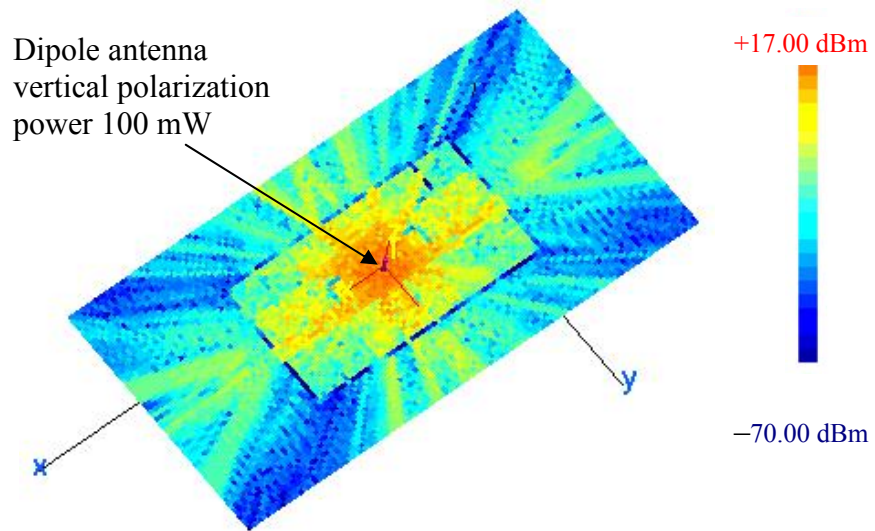


Figure 61. Signal contour for the seventh floor (100 mW source power and antenna on the seventh floor)

The influence of the transmitted power on the propagation and the strength of the signal are obvious in Figures 60 and 61. The maximum power computed in the first figure is 12.35 dBm and, when the transmitted power was reduced to 100 mW, the maximum value in the observation plane dropped to 2.35 dBm. Table 15 summarizes the values of the maximum energy in each floor.

Floor number	Signal level with transmitter power of 1 W	Signal level with transmitter power of 100 mW
1	-75.48	-85.48
2	-59.3	-69.3
3	-48.31	-58.31
4	-34.31	-44.31
5	-18.45	-28.45
6	-5.8	-15.8
7	12.35	2.35
8	-3.45	-13.45
9	-18.01	-28.01
10	-31.25	-41.25
11	-43.07	-53.07
12	-60.52	-70.52

Table 15. Comparison of signal levels for source powers of 1 W and 100 mW

4. Observation Points in a Vertical Plane

A series of cuts were generated in the vertical plane (y - z) to display the shape of signal contour inside and outside of the building as a function of the height. The y - z cuts started at $x = -5$ m and ended at $x = 45$ m. The step size is 10 m. The results are shown in Figures 62 and 63. The maximum signal level for each cut is listed in Table 16.

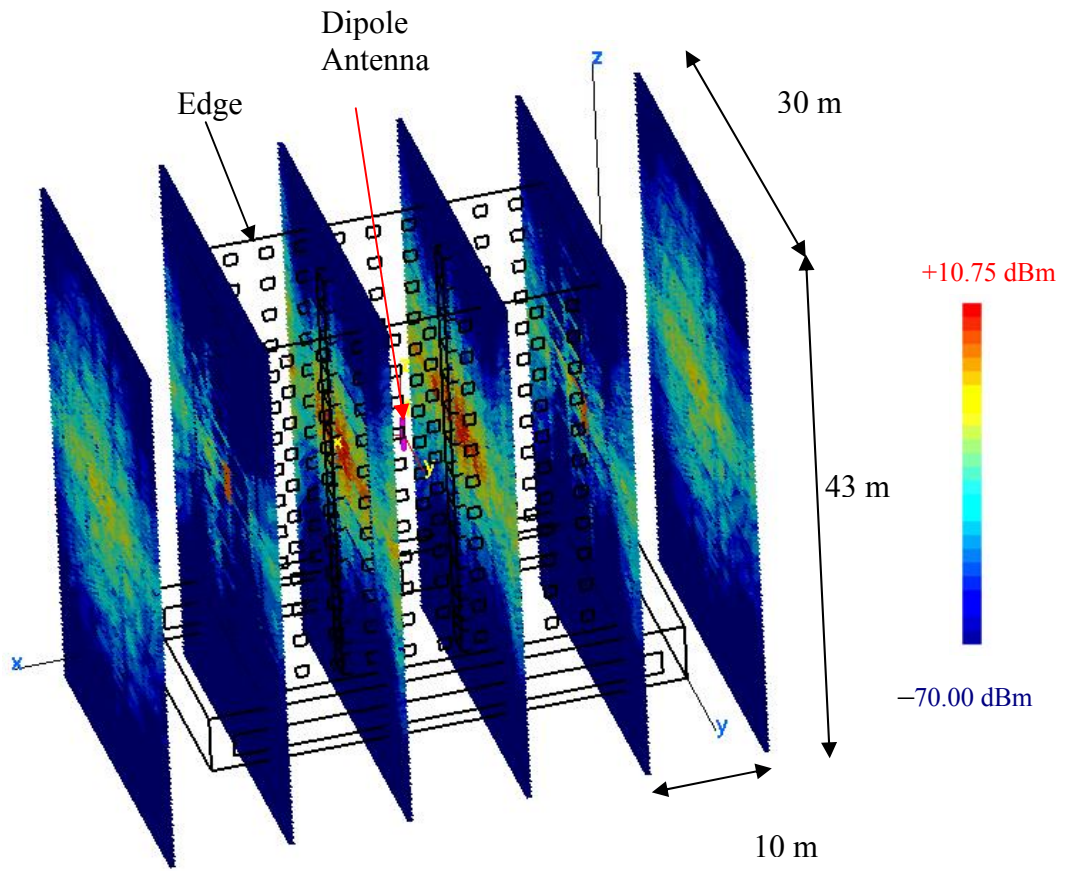


Figure 62. Vertical signal contour (right view)

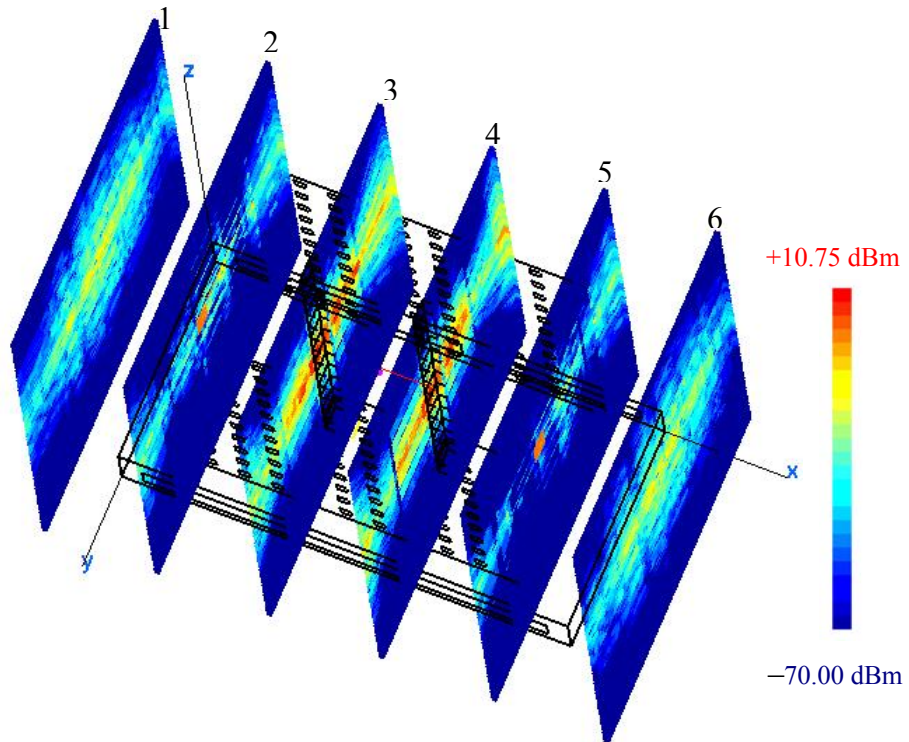


Figure 63. Vertical signal contour (left top view)

Plan number	Position of the (y - z) observation plane ($-5 \leq y \leq 25, -5 \leq z \leq 37$)	Maximum level of signal (dBm)
Cut 1	$x = -5$ m	-10.04
Cut 2	$x = 5$ m	0.554
Cut 3	$x = 15$ m	9.906
Cut 4	$x = 25$ m	10.75
Cut 5	$x = 35$ m	-2.06
Cut 6	$x = 45$ m	-10.95

Table 16. Maximum signal level for each of the six vertical planes

The signal contours shows a high level in planes 3 and 4, both 10 m displaced from the antenna. The levels are generally symmetric with respect to the upper and lower floors.

D. SUMMARY

This chapter started with the simulation of propagation on one floor, and then proceeded to examine all of the floors of a 12 story high-rise. Two different wall material compositions were examined: all PEC, and more realistic wood and concrete. Both opened and closed doors and windows were simulated. Finally the behavior of the signal contours on all floors of the building was compared, as well as the signal distribution in the vertical planes. In the next chapter we summarize the work done in this research and recommend security measures to prevent unauthorized intrusion of wireless system operating in a high-rise building and additional future work.

V. CONCLUSION

A. SUMMARY

This research focused on assessing the performance of wireless communication systems in the 2.4 GHz band inside a high-rise building by calculating the signal levels using the **Urbana** toolset. A CAD model of the high-rise building was generated in **Rhino** and translated into a *facet* file using **Cifer**. Then a series of simulations were run to obtain the signal distribution throughout the building for various antenna locations. Both horizontal and vertical observation planes were used to visualize the contours of the signals between floors. Several types of building materials were examined. The simulation results indicated that the signal levels for a 1-W transmitter could only be detected at the -70 dBm level within two floors (above or below). Even within the two floor range the signal distribution was very nonuniform due to the effects of multipath.

The results indicated that closing doors reduces the signal levels, but only slightly for wood doors. Signals escaped the building through the window and were able to travel between floors via this path. The ray tracing accounted for only single diffraction, and therefore rays diffracted two or more times were not included. An example of such a path is a ray diffracted from a window edge (on the floor where the antenna is located) which travels down the side of the building and then diffracts back into the building at a lower floor. However, it is estimated that this path would suffer at least an additional 10 dB of attenuation over the single diffracted path. Therefore its inclusion should not affect the final contour significantly.

B. CONCLUSION

The variety of the indoor environments influence wireless propagation inside of buildings enormously. Two main WLAN vulnerabilities were evident from this work. First is the spread of the signal outside the building through the windows. Simulations showed that the levels of the signal were sufficient enough to be detected on the ground outside, especially if the access point was located on one of the first three floors of the building. The second vulnerability is the penetration of the signal through ceiling and

floors with concrete material. The attenuation of the signal was about 12 to 18 dB per floor, which allows significant power transmission to the first few floors nearest to the antenna.

Considering the results of all simulations performed, it is possible to state some security guidelines for operating wireless systems in a high-rise building.

1. Place the access point on the highest possible floor to prevent interception at ground level outside or in a publically accessible lobby,
2. Use tinted windows to limit leakage to the outside,
3. Use a metal screening material between floors,
4. Reduce the transmit power of the access point, and
5. Raise the sensitivity of the access point receiver.

C. FUTURE WORK

The task of examining the influence of the antenna pattern on the signal level inside and outside of the building can be the focus of future work. More specific environments can be examined, for example, the inside of a hospital or industrial building. **Urban** has an approximate double diffraction option that can be turned on to model doubly diffracted rays that travel along the outer surface of the building.

APPENDIX

The appendix refers to a sample Urbana input file [9], a table of IEEE 802.11 specifications [14] and a table of material specifications [15].

A. SAMPLE URBANA INPUT FILE [9]

```
# *****
# A---scatterer file,length & freq
# *****
#--- name of scatterer file in ACAD format (e.g. wall.facet)
bldg.facet
#--- length unit:1=inch, 2=cm, 3=meter, 4=mm, 5=mil
1
#--- uniform freq (GHz): start freq, end , nstep
# (nstep=0 means: just do first freq. CAUTION: antenna patterns are
# assumed to be indep. of freq and is calculated at end freq)
2.4 2.4 0
#
# *****
# B--- Antenna Description and List
# *****
#
#---Enter method of describing antennas.
# (1 = here, 2 = file):
1
#---If described in file, enter file name:
dummy.antenna
#---If described here, fill in sections B1, B2, B3.
# If described in file, use dummy data in sections B1, B2, B3
# (specify one dummy antenna type, dummy antenna origin,
# and one dummy item in antenna list).
#
# *****
# B1: Define Antenna Types
# *****
#
# Two lines for each type.
# Line1: type ID, ant code
# Line2: parameters
#
# Type ID must start from 1 and increment by 1 thereafter
#
# Ant Code meaning parameters
# -----
# 1 pattern file filename(ascii)
# 2 dipole length(real)
#
# Antenna Types list:
#
# Enter number of antenna types:
1
# Type #1
1 2
2.5
#
# *****
# B2: Enter origin of antenna coord in main coord
# *****
#
0.0 0.0. .0
#
```

10

```
# *****
# B3: Create Antenna List
# *****
#
# Three lines for each antenna.
# Line1: Type ID, location (x,y,z), power (watts), phase(deg)
# Line2: Local x-axis in main coord.
# Line3: Local z-axis in main coord.
#
# Enter number of antennas:
1
#
# Antenna #1
1 50.0 50.0 30.0 1. 0.
1. 0. 0.
0. 0. 1.
#
# *****
# C---Observation points
# *****
#--- Observation points defined with respect to main coord. system 7.
# Enter method of specifying list of points.
# (1 = here, 2 = file):
2
#--- If points are listed here, enter number of points (kobtot):
1
#--- If listed here (1 above), List xyz of points in main coord 7
# (one point at a line). If 2 above, include one dummy line.
1. 2. -11.00
#--- If points listed in file (2 above), enter name of file.
bldgobv.list
#--- Include direct Tx to observer contribution.
# If you turn on the direct contribution from the transmitter to the
# observation point, computed result will be the total field, which is
# the incident + scattered field. For propagation analysis, this is
# the preferred setting. Otherwise, the result only includes the
# scattered field.
#
# Include direct contribution from transmitter to observation point (rx)
# (1 = yes, 0,2 = no):
1
#--- Compute received power into Rx antenna.
# Urbana always computes field levels at the observation point.
# If you specify an Rx antenna, Urbana will also compute the received
# power and record the results in the (runname).couple file.
# This causes a moderate but slow-down when using the SBR method (below).
#
# Include Rx antenna (1 = yes, 0,2 = no):
0
#--- Rx antenna specification
# Remaining entries in Section C can be ignored if not including
# an Rx antenna.
# Enter antenna type (1 = pattern file, 2 = dipole):
2
# Each antenna type requires additional parameters.
# List of expected parameters follows. Choose one.
#
# Type Description Expected Parameter(s)
# 1 Pattern File File Name (e.g., beam.antpat)
# 2 Dipole Length (in prevailing unit)
#
# Enter parameter(s) on next line:
2.5
#--- Rx antenna orientation
11
# Enter local x-axis of Rx in global coordinates
1. 0. 0.
# Enter local z-axis of Rx in global coordinates
0. 0. 1.
```

```

#
# *****
# D---Theoretical consideration
# *****
#--- Choose method of computation
# 0 = compute fields in the ABSENCE of the scatterer
# 1 = compute fields by SBR
# 2 = compute fields by GO
2
#--- If SBR, select a PO integration scheme at bounce points
# 1 = do integration at first & last bounce points only
# 2 = do so at all bounce points (GTD formulation)
# 3 = do so at all bounce points (PTD formulation)
2
#--- Edge diffraction
# SBR can be enhanced with PTD edge diffraction.
# GO can be enhanced with GTD edge diffraction.
# Add edge diffraction (0,2=no, 1=ILDC (SBR or GO), 3=UTD (GO only)
3
#--- If edge diffraction switched on, enter name of edge file
# (e.g., wall.edge or dummy if edge not included).
bldg.edge
#--- Choose method of ray launch
# 1 = by (baby) facet, achieving a uniform first bounce surface density
# 2 = uniform angular distribution (burst launch)
# (If computation by GO, must select 2 = burst launch)
2
#--- If ray launch by (baby) facet (1 above), enter ray density:
# # rays/wavelength (normally 5-10)
5.
#--- If burst ray launch (2 above), enter angular interval (deg).
# (Typically 0.25 - 2.0 deg)
2.
#--- max permissible ray bounces (normally 5-10)
5
#--- max-voxdepth = max depth of BSP tree (normally 20)
# max-voxl = max facets in each voxel (normally 10)
# (Larger voxdepth & smaller voxl lead to faster ray tracing
# but more computer memory)
20,10
#--- ICOAT for absorbing facets
888
#--- IQMATRIX for divergence factor
# 1 = calculated by Q-matrix
# 2 = ignored except for the spherical wave spread
2
#--- IF using Q-matrix, name target curvature file(e.g. wall.curv)
dummy.curv
#--- IPEC=1 if all pec, =2 if coating present
1
#--- For PEC scatterer, give the magnitude of reflection coeff
# (use 1.0 for ideal PEC, use less for rough PEC--fudging)
1.
#--- IF PEC, the rest coating info is dummy
#--- material reflection is done through a look-up table
# specify the freq interval in GHz for the table e.g. 0.25
# (dummy if input freq less than 51)
0.2
*****
E---coating material
*****
---- number of materials
(NOT including pec, which is identified by ICOAT=0)
(NOT including absorbing facets: ICOAT=28 or 888)
(If 3 material, urbana reads only ICOAT=1-3)
1 <----NCOTOT
--- for each material, identify its boundary type:
iboundary = 1 if impedance boundary
2 if layered slabs with PEC backing
3 if penetrable layered slabs with air backing
4 if penetrable FSS Tx/Refl table supplied by user
5 if same as 2 except using freq-dep ramlib.d

```

```

6 if antenna refl table supplied by user
7 if layers over semi-infinite ground
# for each material, given info by following the templates
^^^ ICOAT=1 ^^^^^^^^^^^^^^^^^^^^^^^^^^^^^^^^^^^^^^^^^^^^^^^^^^^^^^^^^^^^^
--- iboundary
3
--- number of layers over air backing
(1st layer is farthst fr incid field and innermost)
1
--- thick,epsilon(c),mu(c),resistivity(ohm)
6.00 (5.5,-.5) (1.0,0.0) 1e30
(End of regular input file. Leave a few blank lines)
(Rest of file not listed)

```

B. TABLE OF 802.11 SPECIFICATIONS [14]

	802.11b	802.11g	802.11a
Compatibility	IEEE 802.11b compliant. Wi-Fi CERTIFIED*	IEEE 802.11b and 802.11g compliant. Wi-Fi CERTIFIED*	IEEE 802.11a compliant. Wi-Fi CERTIFIED*
Number of Channels	3 non-overlapping	3 non-overlapping	8 non-overlapping (4 in some countries)
Typical Indoor Range	100 ft (30 m) @ 11 MBps; 300 ft (91 m) @ 1 Mbps	100 ft (30 m) @ 54 MBps; 300 ft (91 m) @ 1 Mbps	40 ft (12 m) @ 54 Mbps; 300 ft (91 m) @ 6 Mbps
Typical Outdoor Range (Line of Sight)	400 ft (120 m) @ 11 Mbps; 1500 ft (460 m) @ 1 Mbps	400 ft (120 m) @ 54 Mbps; 1500 ft (460 m) @ 1 Mbps	100 ft (30m) @ 54 Mbps; 1000 ft (305m) @ 6 Mbps
Data Rates	11, 5.5, 2 and 1 Mbps	54, 48, 36, 24, 18, 12, 9, and 6 Mbps	54, 48, 36, 24, 18, 12, 8, and 6 Mbps
Wireless Medium	Direct Sequence Spread (DSSS), 2.4 GHz	Orthogonal Frequency Division Multiplexing (OFDM), 2.4 GHz	Orthogonal Frequency Division Multiplexing (OFDM), 5 GHz

C. MATERIAL SPECIFICATION AT 2.4 GHZ [15]

Material	Real value of the complex permittivity ϵ'_r	Imaginary value of the complex permittivity ϵ''_r
Plexiglas (7.1mm)	2.74	8.77E-04
Plexiglas (2.5mm)	2.5	2.34E-02
Blinds (closed)	3.49	2.08E-04
Blinds (open)	1.96	1.17E-04
Red brick (dry)	5.86	6.83E-01
Red brick (wet)	5.92	6.96E-01
Carpet (back)	1.31	8.76E-04
Carpet (weave)	1.32	7.87E-05
Ceiling tile	1.32	1.90E-02
Fabric	1.49	8.88E-05
Fiberglass	1.02	9.39E-04
Glass	6.38	1.66E-01
Drywall (12.8mm)	2.19	2.43E-02
Drywall (9mm)	2.49	1.06E-02
Light cover (front)	1.66	1.14E-02
Light cover (back)	1.64	1.95E-02
Linoleum (back)	3.04	1.92E-04
Linoleum (front)	3.08	4.47E-03
Fir	2.58	5.23E-01
Particle Board	2.7	2.98E-01
Plywood	2.47	3.15E-01
Stucco (back)	7.3	3.48E+00
Stucco (front)	1.07	4.89E-01
Tiles	3.08	1.81E-01
Tar paper	2.47	9.54E-02

THIS PAGE INTENTIONALLY LEFT BLANK

LIST OF REFERENCES

- [1] "Wireless Hacks Growing Threat," [www.techweb.com/wire/story/ TWB2 004080-3S0003](http://www.techweb.com/wire/story/TWB2_004080-3S0003), August 2004, last accessed November 2004.
- [2] Paul P. Sumagasay, "Vulnerability of WLANs to Interception," Master's thesis, Naval Postgraduate School, September 2002.
- [3] Wee Pin Lim, "Vulnerability of Wireless Point-to-point Systems to Interception," Master's thesis, Naval Postgraduate School, December 2003.
- [4] K. Siwiak, *Radiowave Propagation and Antennas for Personal Communications*, 2nd edition, Artech House, Boston, 2003.
- [5] "Indoor Propagation Issues for Wireless LANs," http://rfdesign.com/mag/radio_indoor_propagation_issues/, October 2004, last accessed October 2004.
- [6] T. Rappaport, *Wireless Communications*, Prentice Hall PTR, NJ, 2002.
- [7] J. C. Stein, "Indoor Radio WLAN Performance," <http://www.netsmith-inc.com/WLANs-in-offices.pdf>, September 2004, last accessed October 2004.
- [8] "Wireless Indoor Antennas," www.wlanantennas.com/indoor_antennas.htm, September 2004, last accessed November 2004.
- [9] "Urbana Wireless Toolset," Science Application International Corporation (SAIC), October 2004.
- [10] J. B. Keller, "One Hundred Years of Diffraction Theory," *IEEE Transactions on Antennas and Propagation*., Vol. AP-33, No. 2, pp. 123-126, February 1985.
- [11] D. A McNamara, C. W. I. Pistorius, and J. A. G. Malherbe, *Introduction to The Uniform Geometrical Theory of Diffraction*, Artech House Inc., Boston, 1990.
- [12] D. C. Jenn, *Radar and Laser Cross Section Engineering*, American Institute of Aeronautics and Astronautics, Washington, 1995.

[13] C. W. Chang, "Radiowave Propagation Modeling using the Uniform Theory of Diffraction"
www.ece.auckland.ac.nz/~p4p_2004/archive/reports2003/pdfs/p9_ccha189.pdf, September 2004, last accessed November 2004.

[14] <http://www.intel.com/business/bss/infrastructure/wireless/solutions/standards.htm>, last accessed November 2004.

[15] <http://www-scf.usc.edu/~robertwi/papers/magis.pdf>, last accessed November 2004.

INITIAL DISTRIBUTION LIST

1. Defense Technical Information Center
Ft. Belvoir, Virginia
2. Dudley Knox Library
Naval Postgraduate School
Monterey, California
3. Chairman, Electrical & Computer Engineering Department
Code EC
Naval Postgraduate School
Monterey, California
4. Professor David C. Jenn
Code EC/Jn
Naval Postgraduate School
Monterey, California
5. Professor Tri Ha
Code EC/Ha
Naval Postgraduate School
Monterey, California
6. Professor Jeffrey Knorr
Code EC/Ko
Naval Postgraduate School
Monterey, California
7. Boukraa Lotfi
Tunisia